WEAR BEHAVIOR OF PVD TITANIUM NITRIDE-COATED TOOL STEELS

Xihong Wang
B.S., Hebei Institute of Mechanical
& Electrical Engineering, China, 1983
M.S., Academy of Machinery Science & Technology
China, 1986

A thesis submitted to the faculty
of the Oregon Graduate Institute
of
Science and Technology
in partial fulfillment of the
requirements for the degree
of Master of Science
in
Materials Science and Engineering

August 25, 1989

The thesis "Wear behavior of PVD titanium nitride-coated tool steels" by Xihong Wang has been examined and approved by the following Examination Committee:

Paul Clayton
Thesis Research Adviser
Professor
Department of Materials Science and Engineering
Oregon Graduate Institute of Science and Technology

Milt Scholl
Research Scientist
Department of Materials Science and Engineering
Oregon Graduate Institute of Science and Technology

Paul Davis
Professor
Department of Applied Physics and Electrical Engineering
Oregon Graduate Institute of Science and Technology

DEDICATION

To my mom and dad for their faraway love and encouragement.

ACKNOWLEDGEMENTS

First thanks to Dr. Paul Clayton, my thesis advisor, for his support and guidance. I am most indebted to Dr. Milt R. Scholl for his instruction and endless patience during the course of this work.

Dr. Paul R. Davis is greatly acknowledged for being a member of my thesis examination committee. I would also like to thank Dr. Mike Bozack, Department of Physics at Auburn university, for the XPS work.

Personal thanks are extended to John, Deva, Dan, Partha, Chen, Vivek, and other people of the Department of Materials Science and Engineering for their help and friendship while this work was conducted.

Table of Contents

List of Tables

List of Figures

ABSTRACT

WEAR BEHAVIOR OF PVD TITANIUM NITRIDE-COATED TOOL STEELS

Xihong Wang

Oregon Graduate Institute of Science and Technology, 1989

Supervising Professor: Paul Clayton

Titanium nitride films deposited by physical vapor deposition (PVD) have received great interest as wear resistant coatings. In spite of many successful applications, especially on metal cutting tools, the mechanisms by which these coatings fail or degrade are poorly understood. The wear behavior of commercial titanium nitride coatings prepared by two different PVD evaporation processes were studied using the Dry Sand Rubber Wheel (DSRW) test and wood cutting tests. Their performance was compared with an electroplated chromium coating.

Titanium nitride coatings were deposited on high speed steel substrates by two commercial PVD coating vendors. One vendor used an arc evaporation PVD process while the other used electron-beam evaporation. The thickness of these commercial titanium nitride coatings varied from 0.5 to 2.4 μm depending on the side of the sample. The thicker titanium nitride coating showed a higher wear resistance than the electroplated chromium coating. However, the thinner

titanium nitride coatings did not perform better than the electroplated chromium. Macroparticles distributed on the titanium nitride coating surface were found to influence the initial deterioration of the thicker titanium coating, while microcracking observed on the surface of the thinner titanium nitride coating is believed to enhance coating removal. The electroplated chromium was found to degrade by uniform grooving wear in contrast to the titanium nitride coatings which deteriorated predominately by a spalling process. There was no difference in deterioration behavior or wear resistance observed between the arc-evaporated titanium nitride coating (0.7 μm thick) and the thin titanium nitride coating (0.5 μm thick) produced by electron-beam evaporation.

The ranking of wear resistance in the wood cutting test among the different types of coatings was different from that of DSRW testing; with the Cr-coated cutters having the highest wear resistance, the Multi-Arc arc-evaporated TiN coating the second highest, and the Balzers electron beam evaporated TiN coating the lowest wear resistance. Coating deterioration was also found to be different from that observed in the DSRW test. Microcracking was not observed on the coating surface. The higher hardness of the abrasives used, the higher shear forces acting on the vicinity of the saw chain cutter tip, and substrate (AISI 8660) softening possibly accounted for the performance of titanium nitride coatings in the wood cutting testing.

More extensive evaluation of the coating deterioration in both tests is recommended to realize a full understanding of these coatings and their behavior in abrasive environments.

1. INTRODUCTION

1.1 Ceramic Films

The ceramic coating market has been growing rapidly in the last decade. The market for 1988 is valued at 310 million dollars, and is expected to grow 9.5 percent annually to 488 million dollars by 1993[1]. Advanced ceramic thin films, including nitrides, carbides, oxides and borides, are valued for their thermal, wear and corrosion resistance, electrical insulation properties, high magnetic permeability and special optical properties[2]. These characteristics are useful for a wide range of applications, such as decorative films on glass for architectural structures and automotives[3], medical devices[4], diffusion barriers for microelectronic components[5-7] and solar cells[8], as well as microelectronic packaging[9].

Ceramic thin films are particularly promising in the microelectronic industry. They possess a combination of electrical, thermal, mechanical, and dimensional properties unmatched by any other group of materials. For example, ceramic thin films have dielectric constants from 4 to 10,000, thermal expansion coefficients matching silicon (30×10^{-7}/°C) or copper (170×10^{-7}/°C) and thermal conductivities ranging from one of the best insulators (such as glass-ceramics, 5W/mK, formed by controlled crystallization of glass) to greater than aluminum (220W/mK)[9]. Recent technological breakthroughs have opened the door for high temperature ceramic thin film superconductors.

The current ceramic coating market is dominated by aerospace and cutting tool applications, which account for 85 percent of the market[1]. In the United States, about 85 percent of carbide tools and 15 to 20 percent of tool steels are coated with ceramic thin films, which enhance tool life by a factor of 2 to 10 times and sometimes higher[10,11].

1.2 Thin Film Deposition Techniques-PVD and CVD

Ceramic films can be classified as thin films, 1-10μm thick, and thick films, 10-1000μm thick. Thin ceramic films are deposited by two principal techniques: chemical vapor deposition (CVD) and physical vapor deposition (PVD).

CVD may be defined as a reaction of volatile components at the surface of a substrate with the formation of a solid surface layer (coating) and volatile reaction products. The reaction is controlled by the thermodynamic equilibrium which depends on vapor pressure and temperature. The reaction takes place in a reactor which contains the substrate. The deposition of TiN by CVD is normally done within the temperature range of 850°C to 1200°C. A typical chemical reaction is as:

$$TiCl_4,\ N_2,\ H_2 \rightarrow TiN,\ HCl,$$

in which titanium tetrachloride, nitrogen, and hydrogen are reacted in a furnace chamber at high temperatures, forming titanium nitride on the substrate surface and excess hydrochloric acid as reaction products.

PVD may be defined as the condensation of a flux of atoms, clusters of atoms, or ionized particles on a substrate in a vacuum. The PVD processes

may be categorized (Fig. 1) as either evaporation or sputtering[12,13].

In the evaporation process [Figure 1(a)], vapors are produced from a source material (titanium when depositing TiN) which is heated by direct radiation, eddy current heating, electron-beam bombardment, lasers, or an electrical discharge. The vapor consists largely of single atoms or clusters of atoms. The process is usually carried out in vacuum of 10^{-4}~10^{-6} torr (containing N_2 gas when depositing TiN)[14], at which pressures the mean free path of a gas atom (i.e. the average distance travelled before it suffers collision with another atom) is of the order of 1 to 100m. As this is very much greater than the typical chamber dimensions, an atom evaporating from a source will travel in a straight line prior to condensation on the substrate and so the process is essentially one of line-of-sight transport[15]. Except in those cases where ionization is present, the energy of the vapor particles is merely that necessary for evaporation[14].

In the sputtering process [Fig. 1(b)], positive gas ions (usually argon ions) produced in a glow discharge or neutral atoms (gas pressure 2×10^{-2} to 15×10^{-2} torr) bombard the target material (a titanium cathode when depositing TiN), dislodging groups of atoms that then pass into the vapor phase and deposit onto the substrate.

Ionization assisted evaporation, also known as ion-plating, is in fact an evaporation process with the addition that a low pressure gas discharge is maintained during coating condensation (Fig. 2). In this process, the vaporized material passes through a gaseous glow discharge on its way to the substrate, with some of the vaporized atoms becoming ionized. The glow discharge is pro-

duced by biasing the substrate to a high negative potential (2 to 5 kV) and admitting a gas, usually argon, at a pressure of 5×10^{-3} to 0.2 torr into the chamber. The substrate is bombarded by high-energy gas ions which helps to remove gaseous impurities, which is desirable for producing better adhesion and lower impurity content in the coating[15]. Ionization assisted evaporation (Ion-plating) was the first technique among the family of plasma (or ionization)-assisted techniques.

The deposition rate of the sputtering process is lower ($\simeq$0.1μm/min) than that of the evaporation process where a deposition rate as high as 75μm/min has been reported, and 2μm/min can generally be obtained[14]. Sputtering is an inefficient way to induce a solid-to-vapor transition. A typical yield for the sputtering process is one atom for each 500 eV argon ion incident on the metal surface[15]. The energy of the bombarding ions in the sputtering process is sufficiently high to overcome the binding energy of any substrate lattice site and so that the technique can be used for coating with a wide range of materials. Thus, the source (also called 'target') can be of an alloy or compound or even a pseudo-alloy consisting merely of a mixture of the powdered constituents[14]. The surface roughness of the coating produced by evaporation is generally higher than that by the sputtering process.

Both evaporation and sputtering can be combined with additional chemical reactions, gas discharge, and negative bias applied to some parts of the system. Among these techniques, the plasma (or ionization) assisted technique has been introduced into all commercial processes. Further information regarding process physics and apparatus can be found elsewhere[16-24]. Figure 3 presents a

hierarchy of PVD processes[25]. Available commercial PVD processes include Magnetron Sputtering by Leybold-Heraeus (FRG), Arc Evaporation by Multi-Arc (USA) and Electron Beam Evaporation by Balzers (USA/Leichtenstein)[12]. The Balzers company utilizes a system which incorporates an electron source operating under medium vacuum conditions. Precise process details (beyond their patent specifications) are not available for publication. In the USA the technique currently favored for TiN deposition appears to be that based on arc evaporation[12]. An arc evaporation was reported to be able to generate a much higher degree of ionization and hence higher deposition rate than other physical vapor deposition processes[21].

PVD vs CVD

CVD is generally carried out at higher vapor pressures and higher temperatures than PVD. Because of the high deposition temperature, an additional hardening and tempering of tool steel substrates is usually necessary after CVD. The deposition rate can be much higher for PVD ($>0.1\mu m$/min) than for CVD ($0.01\sim0.1\mu m$/min). Hard compounds are formed with both processes. By CVD, single, double, or triple layers are formed, such as TiC, TiC/TiN, TiC/TiN/Al_2O_3, and others. With PVD, in most cases, single layers of TiN are deposited[25]. Considering economics and operation, CVD is relatively low cost and simple compared with PVD.

The formation of a deposit involves two steps:

(a) synthesis or formation of the species to be deposited and

(b) growth of the deposited after condensation.

In CVD, these two steps take place at the same time on the substrate under a specific set of processing conditions. Hence, these two steps cannot be independently controlled. On the other hand, in the PVD process, these two steps are essentially independent of each other, and the process parameters for each step can be separately controlled. Thus, one can control the rate of formation or the composition of the vapor species and independently choose the temperature of deposition, which is a most important process variable since it, in turn, controls the microstructure and mechanical properties of the deposit. This feature, along with the ability of depositing a wide variety of materials, illustrates the great versatility of the PVD process and its increasing appeal for the future. Furthermore, with the PVD process, there are no effluents, such as large amounts of gaseous products. This is a significant ecological and economic factor, in view of long-term environmental concerns, in favor of PVD over CVD, which justifies the generally higher capital equipment costs of the PVD process[15].

In spite of all these advantages of PVD over CVD, the commercialization of PVD has not occurred as rapidly as anticipated. The slower growth in development is directly related to the technical problems associated with the process control and the variability of coating microstructures and properties. The main problems can be further listed as follows[12]:

(a) repeatable deposition rate

(b) thickness variations

(c) control of macroparticles (detrimental to the performance and surface finish of components)

(d) stoichiometry and phase non-uniformity (metal-rich nearer to the source)

(e) preferred orientation control

(f) ionization enhancement and heating

(g) uniform bombardment and heating when components of different size are being coated simultaneously

(h) cooling problems.

Continued research is aimed at characterizing these coatings, increasing the knowledge base, and developing the technology required to ensure the production of reliable, reproducible, and cost-competitive ceramic coatings.

Research work conducted in the field of PVD thin film can be illustrated in Figure 4, which can be categorized as:

(a) the relationship between factors involving process parameters, such as gas pressure, current density, applied power, metal to gas ratio, substrate temperature, substrate bias, deposition rate, source to specimen distance, etc., and those involving coating integrity, microstructure such as grain morphology, defect distribution and density, interface structure, stoichiometry, phase constituent, thickness, residual stress, surface texture and roughness[18, 21, 24, 26-46];

(b) the relationship between factors regarding process parameters and those concerning coating properties or performance, such as hardness, adhesion, electrical and optical properties, wear and corrosion resistance,

etc.[21,24,26,29,31-34,37,45,47];

(c) the relationship between coating microstructures and properties or performances[21,26,29,31-34,37,45,48-55].

So far the majority of research work conducted in this field has been related to the process parameters.

1.3 Selection of Coating Materials

A large variety of coatings can be grown by PVD processes. The criteria for selecting a particular coating material depends on the substrate to be used as well as the actual application. Thus, there is a need for a fundamental understanding of both coating/substrate interactions and interactions between the coating and its environment during use. Examples of parameters which must be considered when selecting hard coatings are adhesion of the film to the substrate, effects of both extrinsic and intrinsic stresses on the internal strength, and the hardness of the coating. In many wear applications, severe constraints are placed on the coating/substrate composite. For example, in cutting applications very high force and high temperatures develop in the vicinity of the cutting tip or edge[56,57]. One most important requirement for a hard coating would be that the coating adhesion to the substrate were sufficient to withstand these forces.

Residual stresses are found in thin films and believed having a great influence on coating adhesion[51,58-63]. The internal stresses in thin films consist of two components: intrinsic and extrinsic (thermal) stresses. The intrinsic

stress originates from the growth process as a result of ingrown defects or structural mismatch between film and substrate, while the thermal stress originates from the difference in the thermal expansion coefficient of the film and the substrate[51]. Thermal stresses are an important consideration for coatings grown at high temperatures, and can be either tensile or compressive but tensile stresses are in general most damaging[56,57]. The thermal stress in the coating after cooling from the deposition temperature are tensile when the thermal expansion coefficient of the coating material is larger than that of the substrate material. Thermal expansion coefficients together with other parameters of some typical coatings and substrate materials are given in Table I[60,64]. Both the thermally generated stresses and those caused by the difference in elastic properties between the coating and substrate should be made as small as possible by choosing optimum coating substrate combinations. The intrinsic stresses can be either tensile or compressive in nature depending upon the deposition conditions[64-66].

These stresses result in an increase in the elastic strain energy stored in the film, which acts at the coating/substrate interface where it may cause spalling when it exceeds the interfacial fracture energy. High residual stresses can also cause cracking in the film or the substrate, or cracking at the substrate coating interface[15]. The coating adhesion must be sufficiently high that the intrinsic and extrinsic stresses do not result in delamination at the coating/substrate interface. For films grown by CVD, a mixed interfacial zone generally develops due to interdiffusion since high temperatures and low deposition rates are used. This gives rise to a strong metallurgical bond resulting in high adhesion

provided that no brittle phases are formed in this interfacial zone. During PVD, which is normally carried out at much lower temperatures than CVD, a graded interfacial zone can be formed either by specifically depositing an interfacial layer[53] or by using ion bombardment to promote collisional mixing at the interface, leading to high adhesion[64,67].

For PVD coatings grown at low temperatures, the adhesion can also be improved by using substrates which are structurally similar to the coating material. A structural and chemical matching between coating and substrate results in a low interface energy and thus promotes high adhesion[42,53]. For example, Helmersson *et*al.[37], observed that as the surface density of MC-type carbides in the substrate increases, adhesion increases. This is because MC (a≃4.18 angstrom) carbides have the same structure as TiN (NaCl B1), with a lattice mismatch of only 1.6% with TiN (a=4.24 angstrom).

In many wear applications, the hardness of the coating is of primary interest. For example, in abrasive wear applications the hardness of the coating has to be higher than the hardness of the abrasive particles themselves[57]. This can be achieved either by choosing a coating material whose intrinsic hardness satisfies the requirement or by modifying the microstructure of the coating so that the desired hardness is obtained[64].

1.4 TiN

Ceramic coatings with good wear properties include TiC and TiN as well as multi-layer coatings, such as TiC/Al_2O_3, $TiC/TiN/Al_2O_3$, and

$TiC/Al_2O_3/TiN$[11]. Among these TiN has been the most widely used commercial ceramic for wear resistance applications. The most successful application area for TiN so far is that of coatings onto various cutting tools. Thin films of about 2-10μm are found to increase the tool life by many times[68]. The use of titanium nitride as diffusion barriers[7] and solar cells[8], for selective transparent films and for high temperature photothermal conversion[69,70] has also been investigated.

In spite of the many application areas there is still a lack of knowledge of how these films grow and of how the resulting structure and properties depend on the growth conditions. Since the films are grown using different techniques and process parameters, wide variations in growth conditions and thus in structures and properties exist. Many of the structural features reported were obtained from X-ray diffraction and scanning electron microscopy (SEM) studies. Only limited microstructural information has been obtained by transmission electron microscopy (TEM) studies[29,32,33,38,39,42,71].

The Ti-N phase diagram (Fig. 5)[43,72] shows that at room temperature, stable phases vary from hexagonal α-Ti to tetragonal ϵ-Ti_2N (TiO_2 type), to fcc δ-TiN (NaCl type). The mononitride phase TiN is stable over a composition range from N/Ti = 0.6 to N/Ti = 1. N/Ti ratios as high as 1.67 in thin films have been reported[73] whereas the maximum bulk values reported are N/Ti=1.16[74]. The TiN phase which has the NaCl structure has a lattice parameter of 4.24 angstrom at the stoichiometric composition[74]. Multi-phase films containing ϵ-Ti_2N and α-Ti have also been reported[40,43,73-75]. The hardness of bulk TiN is about 2000 Kg/mm^2[76], whereas the reported thin film

hardness varies markedly, ranging from 340 Kg/mm^2 to 4000 Kg/mm^2[22,24,25,28,32,33,64,73]. The high intrinsic hardness can be related to the high cohesive energy, short bond length and a high degree of covalent bonding[64]. The variation in hardness is possibly due to the hardness measurement techniques employed[25], as well as thin film microstructure, stoichiometry, defects, impurity and grain size[64].

The grain size in TiN films, as determined from X-ray line broadening, is generally below 1000 angstrom if the films are grown at temperatures below approximately 600°C. The grain size depends on factors such as the substrate temperature and ion bombardment which affect the growth parameters. An increased substrate temperature leads to a higher mobility of adatoms during growth and also to an increased migration of grain boundaries, factors that both increase the grain size. If the films are exposed to ion bombardment during growth, the grain size is normally found to decrease as the energy of the ions is increased. A higher energy results in more defects generated in the surface thereby increasing the number of preferential nucleation sites and thus decreasing the grain size[64].

Although extensive work has been performed on the wear behavior of titanium nitride thin films prepared by PVD[10,77-94], only limited work has been conducted on coating deterioration mechanisms. The work conducted by Fenske *et al* based on a lathe turning test[91] and Hedenqvist *et al* with a pin-on-ring laboratory test[94] indicated that coatings failed by the softening of the high speed steel substrate and subsequent microfracture of the coating. However, Hedenqvist *et al*[94] also noted that the coating was removed by interfacial

spalling when coated tools slid against austenitic stainless steel instead of plain carbon steel. Clayton and Scholl's work demonstrated the detrimental effect of coarse nodules on the coating surface on the initial wear of an arc evaporated titanium nitride coating[85]. It was illustrated by Erdemir[90] that the rolling contact fatigue (RCF) characteristics of a TiN-coated bearing steel varied with the coating thickness under different load conditions.

It was shown by Rickerby[93] that coating wear mechanisms varied with coating thickness during abrasive wear. Thin coatings failed by localized detachment of the film at the intersections of the plastic grooves formed by the abrasive particles. Thick coatings supported the contact stresses elastically and degrade by microchipping or polishing mechanism with little or no deformation of the underlying substrate. Under severe abrasive wear (a non-resilient vitrified wheel was used instead of a resilient wheel), thick coatings failed by a cohesive fracture mechanism.

Bull[89] found variation in coating wear mechanisms with deposition parameters such as substrate bias which, in turn, can alter the coating microstructure and residual stress level. An ion-plated titanium nitride coating deposited under low substrate bias which produced an open columnar microstructure with low density and hardness degraded by microchipping. With increasing substrate bias, much denser coatings were produced which resulted, initially, in better resistance to abrasive wear through increased load support. However, these improvements in coating microstructure resulted in higher levels of internal stress which gave rise in low adhesion, and eventually, led to a decrease in wear resistance.

These experimental results demonstrate that the coating wear mechanism may vary with differences in deposition parameters, coating microstructure, substrate materials and testing conditions. More extensive work therefore has to be carried out before a thorough understanding of coating wear mechanisms can be achieved.

1.5 Scope of This Study

Titanium nitride films deposited by physical vapor deposition (PVD) have received a large interest as wear protective coatings. These coatings are now commercially available with the major application being on various types of metal cutting tools[25,31,48,49,77,83,84,91,95,96]. One of the inherent advantages of PVD over other techniques, such as chemical vapor deposition (CVD), is its low deposition temperature[11,25]. This is particularly useful when substrate softening and distortion must be controlled. In spite of these advantages and successes, the mechanisms by which these surface coatings fail or degrade are poorly understood, and the interrelationship between the coating microstructure and tribological behavior has not been established.

For many years, the life of saw chain cutters in professional logging operations has been dependent upon the benefits derived from chromium plated clearance faces[97]. Klamecki, in a comprehensive review of the wear of wood cutting tool in 1979[98], indicated that abrasion was the primary wear mechanism of most wood cutter edges, later confirmed by Scholl and Clayton's work based on a field test[97]. A PVD TiN coated tool might be expected to exhibit a longer

life than a chromium-plated one as titanium nitride (Vickers-hardness 2000) is much harder than chromium (1100 HV_{30}). A long term environmental concern is also an important factor in considering the PVD technique as an alternative for electroplating technique. Potential hazards that attend the chromium-plating process are associated with various chemicals used in (a) acid and alkaline cleaners, (b) vapor degreasers, and (c) the chromium plating bath. The mixing of certain of these chemicals can result in a violent reaction. Additionally most are toxic poisons. Chromic acid waste has to be either recovered or destroyed depending on the cost and space requirements. Strict regulations are being enforced by state and federal authorities regarding the allowable limits for chromic acid waste that are dumped into rivers, lakes, and sewage disposal systems. However, there is no such waste to be handled when depositing TiN with PVD process[13].

The purpose of this experiment is to

1. investigate the abrasive wear behavior of commercial titanium nitride coatings.
2. seek alternatives for hard chromium coating prepared by electroplating on saw chain cutters.

This study examined the tribological characteristics of thin films by Dry Sand Rubber Wheel (DSRW) and wood cutting tests. In the present experiments, titanium nitride coatings were commercially prepared by two companies, Balzers Inc. and Multi-Arc Inc. Both companies use evaporation techniques. Balzers, however, uses an electron beam while Multi-Arc uses an arc to eva-

porate source materials. For comparison and analysis regarding to coating wear resistance and degradation mechanisms, samples were also commercially electroplated with hard chromium (by Precision Tool for DSRW test and Omark Industries for wood cutting tests).

As an initial objective of this program was to examine the use of the PVD titanium nitride coating as a replacement for chromium coating on saw chain cutters (Fig. 6), wood cutting testing was performed using a lathe-based laboratory test[99]. DSRW test was selected since it is one of the simplest laboratory abrasive testing methods. Although both tests can be considered as abrasive, the wood cutting test is more severe than DSRW test as more constraint, higher loads and harder abrasives were applied. In addition to the investigation of coating wear behavior, surface and cross-section metallurgical characteristic evaluation by SEM, coating microstructure examination by TEM, phase constituents and surface orientation determination by X-ray diffraction, coating stoichiometry by XPS, residual stress analysis and surface roughness measurement were attempted to assess the properties of the titanium nitride coatings.

2. EXPERIMENTAL

2.1 Substrates

For the DSRW abrasive test three types of materials were used as the substrates: (1) high speed steel (standard tool material manufactured as lathe cutoff tools) which was in the as-received quenched and tempered condition, before being deposited with titanium nitride; (2) O1 tool steel which was in the as-received quenched and tempered condition, before being deposited with titanium nitride; and (3) AISI 1095 steel which was hardened before being deposited with hard chromium. The size of the coupons for DSRW was 1"×3"×1/4".

For wood cutting tests a single type of material was used. As-received saw chain cutters made of 8660 steel were austempered before being deposited with titanium nitride and chromium coatings. The geometry of as-received saw chain cutters is shown in Figure 6.

Chemical analysis of substrate materials was conducted by ESCO, a local steel company. The compositions of all the substrates tested in this experiment are listed in Table II. The hardnesses of substrates were also tested before and after coating deposition.

2.2 Coating Deposition

Samples made of HSS for the DSRW test and saw chain cutters made of 8660 for the wood cutting test were deposited with titanium nitride coatings by two commercial companies, Balzers and Multi-Arc. As mentioned in the previous chapter, both companies use evaporation sources, with the difference that Balzers uses an electron beam while Multi-Arc uses an arc to evaporate the titanium source material. Coupons made of O1 tool steel for DSRW test were also sent to Multi-Arc for titanium nitride deposition.

Samples made of 1095 for the DSRW test were electroplated with hard chromium by Precision Tool, a commercial company, while saw chain cutters made of 8660 for the wood cutting test were coated with hard chromium by Omark, the manufacturer of the saw chain cutters.

Table III lists substrates used and the commercial companies.

2.3 Coating Structural Characterization

Coating surfaces and cross-sections were evaluated using a JEOL JSM-35 Scanning Electron Microscope. Samples for evaluation were sectioned normal to the coating surface of the coupons for the DSRW test and to the clearance face of saw chain cutters for the wood cutting test. They were thoroughly cleaned and nickel plated before being mounted. To get the best cleaning effect before nickel plating, samples were first ultrasonically cleaned in a solution of acetone and ethanol for about 5 minutes. They were then put into a solution of hot

sodium hydroxide for 15 minutes to remove the surface oxides. NaOH particles were dropped into water contained in a beaker set on a hot plate at a warm temperature for about 15 minutes before samples were put in. In this way, the NaOH was completely diluted by the water. The samples were then cleaned in the flowing water for one minute and immediately put into the nickel plating bath to avoid any oxidation in the air. In the final step of sample polishing, the coating surface was held perpendicular to the wheel rotation. This step should not last more than 30 seconds for edge retention. Sample thicknesses were measured by observations of the polished cross-section in the SEM.

Slices 3 mm×3 mm×0.5 mm for TEM work were cut parallel to the coating surface from HSS coupons (1"×3"×1/4") used in the DSRW test. They were glued onto a 1 cm (height)×1 cm (diameter) glass base with the coating side facing the glass. They were ground with #600 SiC metallurgical grinding paper from the substrate side until about 30μm thick. The samples (still glued on the glass) together with the glass base were put into a solution of 10%bromine and methanol until the substrate was dissolved. The high speed steel substrates and titanium nitrides films could be distinguished according to their colors. The former showed black in the solution while the latter always showed bright yellow. A free standing titanium nitride film could be finally obtained after the epoxy between the glass and the film was dissolved. This was done by putting the glass base with the film on it onto a filter paper which was then rinsed with acetone. The free standing films were thinned until perforated by argon ion milling for observation under TEM. The ion-milling machine (ION TEC B306) was manipulated at an acceleration voltage of 4 ~ 6 kV, target

current of 0.2 ~ 0.8 mA and ion beam incident angle of 15°. A Hitachi H800 Scanning Transmission Electron Microscope was operated using an acceleration voltage of 200 kV. Some samples were so thin that they could be directly put into TEM for observation without being ion-milled.

Coating Stoichiometry (by XPS)

Coating stoichiometry was analyzed by a Kratos XSAM-800 Multitechnique surface analysis system (Arburn University). The equipment was operated with a total X-ray power of 300 W and incident X-ray current of 50 nanoamps. Mg K_α (1253.6 eV) was used for exciting radiation and a non-monochromatized dual anode was employed as X-ray source.

Phases and Surface Texture (by XRD)

Bar coupons for DSRW were sectioned into sizes of 1×1 cm^2 for X-ray diffraction analysis. Both sides of titanium nitride plated samples were examined using SIEMENS D500 Powder X-ray Diffractometer. CuK_α ($\lambda = 1.542$ angstrom) radiation was used. The machine was operated at a scanning speed of 0.01°/sec, power of 40kV×3.18A and a scanning angle ranging from 30° to 130°.

Residual Stress Analysis

Qualitative analysis on the state of residual stresses in the thin films was attempted using observations of the film shape after the HSS substrate was dis-

solved. Sample preparation was same as that for TEM work. As the residual stresses relax without the restraint of the substrate, the thin film will twist when its substrate is dissolved. When viewed from the substrate side, convex films indicate the existence of compressive stresses while concave ones indicate the opposite.

Surface Roughness

The surface roughnesses of bar coupons for DSRW test were measured by a surface roughness tester (Mitutoyo Surftest 401). A cutoff length of 0.25μm and frequency of 5 were used.

2.4 Dry Sand Rubber Wheel Test

Figure 7 shows a schematic diagram of the test apparatus. Except for the number of wheel revolutions, all the testing conditions followed the ASTM G65 procedure C^{100}. ASTM procedure uses a fixed one hundred revolutions. Testing was performed at a wheel rotation speed of 200 rpm and normal load of 130N. AFS 50/70 (sizes 212 ~ 300μm)[100] silica sand (hardness ≃ HV 800) was used as the abrasive with the sand flow rate controlled between 250 and 350g/min. The diameter of the rubber wheel (≃9") was measured periodically during the test. In order to obtain more data and observe the coating deterioration phenomena during the wear process, samples were unloaded from the test apparatus after intervals of 5 to 10 wheel revolutions (about 12 to 25 ft of path length) in the initial stages of testing, and at longer intervals later.

They were cleaned ultrasonically in a mixed solution of acetone and alcohol and dried immediately prior to weighing after each interval. A balance (METTLER AE240), which has a sensitivity of 1×10^{-4}gm in the range of 200 gm and 1×10^{-5}gm in the range of 40 gm, was used for weight measurement. For each sample, the test continued until the coating on it was completely removed and a linear wear rate was observed. The wear resistance was evaluated by weight loss plotted against path length which was converted from the number of wheel revolutions. The wear surfaces of the testing samples were recorded by a scanning electron microscope.

To evaluate the reproducibility of the testing, A588 mild steel was tested prior to and during the tests on coated samples.

2.5 Wood Cutting Test

Figure 8 is a photograph of the lathe-based testing apparatus. Wood rotational speed was fixed at 630 rev/min for all tests. The cutters were held in the machine to enable cutting to take place perpendicular to the lathe axis (cross-feed mode) at a cross-feed speed of 0.00375 in/rev. Longitudinal movement (longitudinal mode) was controlled manually. The actual linear cutting speed varied with the wood diameter, 500-920 ft/min, as cutting progressed in the cross-feed mode. A commercial coolant sprayer was used to spray the wood with a solution of 1 wt%Al_2O_3 (LECO optical finishing powder, sizes $\simeq$ 5μm and hardness $\simeq$ HV 2000) in water to simulate field environment of wet wood-cutting[99]. Douglas Fir, 6"$\times$6" quartersawn heartwood, was obtained from a

local lumber yard. They were turned from the square stock into rounds of approximately 5.3 inch diameter for use in the test. For cutting in the cross-feed mode, the starting and finishing diameters were measured and a count was made of the number of cuts. A short computer program[99] was employed to calculate the total path length, taking it to be a series of concentric rings, each smaller than the previous one by twice the feed rate. After each interval, approximately 5,000 ft of cutting path length, the cutter was removed and cleaned for weight measurement by a balance (METTLER AE 240) and examination of the cutting edges and tips by SEM. The cumulative weight loss for each of the test cutters was plotted versus cutting path length and the wear resistances were evaluated by weight loss. Three cutters of unplated and plated by each coating type, Cr, TiN from Balzers and TiN from Multi-Arc were evaluated.

3. RESULTS

3.1 Substrate Hardness

The hardnesses of substrate materials before and after coating deposition are listed in Table IV. The high speed steel used in DSRW test showed little change after titanium nitride coating deposition. The hardness of O1 tool steel for the DSRW test was decreased from HRC 60.0 before titanium nitride coating deposition to HRC 52.5 after the deposition. The hardness of 8660 for wood cutting test was not altered after chromium coating deposition. However, it dropped from HRC 53.6 before coating deposition to HRC 51.6 after titanium nitride coating deposition by Multi-Arc and to HRC 47.6 after titanium nitride coating deposition by Balzers.

3.2 Coating Structural Characteristics

Cross-sections

Figure 9 shows the cross-sections of some specimens for DSRW test: (a) sample cut from TiN-coated HSS (coupon #H3) by Multi-Arc ($\simeq$ 0.7μm thick), (b) sample cut from TiN-coated O1 tool steel (coupon #O2) by Multi-Arc ($\simeq$ 1.4μm thick), (c) sample cut from TiN-coated HSS (coupon #H9) by Balzers ($\simeq$ 2.0μm thick), and (d) sample cut from Cr-coated 1095 (coupon #C1) by Precision Tool ($\simeq$ 10.4μm thick). The thickness of bar coupon #H7 coated with

TiN by Balzer was approximately 2.4μm in one side and 0.5μm in the other side. Samples cut from HSS bar coupons coated by Multi-Arc were found to have the same thicknesses on both sides.

The cross-sections of saw chain cutter clearing face were examined by SEM. The coating thicknesses at those positions ranged from 1.9 to 2.1μm for the cutters coated with titanium nitride by Multi-Arc, 1.0 to 1.5μm for the cutters coated with titanium nitride by Balzers and 9μm for the cutters coated with chromium by Omark.

Microstructures by TEM

Free standing thin films were obtained after their substrates were dissolved. Very thin films ($\simeq$ 0.5μm) without substrates were extremely brittle and in many cases were broken into many tiny pieces. These small pieces were stuck on to copper holders and directly put into TEM for observation. Figure 10(a) is a bright field photograph taken of a film with 0.5 μm thickness from a TiN-coated HSS (coupon #H7) by Balzers. The picture shows sharp grain boundary along which no defects such as voids reported by Hibbs and Sundgren *et al* were observed. Figure 10(b) is a bright field photograph taken of a sample from a TiN-coated HSS coupon (#H1) by Multi-Arc. No details can be seen due to the poor image quality.

Free standing thick films without substrates or films with substrates ground to thickness less than 15μm were attempted to be thinned by ion-milling but no useful samples were obtained. The films under ion bombard-

ment warped.

XPS

The intensity peak area ratio of Ti/N was 4.17 for the thin TiN coating from Balzers, 3.97 for the thick coating from Balzers, 3.70 for the coating from Multi-Arc. No direct atomic ratio of Ti/N was obtained.

XRD

Figure 11 is the X-ray diffraction diagrams on the bar coupons coated with TiN by Multi-Arc and thick TiN by Balzers which showed the following results:

(1) titanium nitride coating (thick side) from Balzers and titanium nitride coating from Multi-Arc had a strong 111 orientation.

(2) δ-TiN was the only phase constituent in both types of titanium nitride coatings.

Upon realizing the difference in coating thickness on the two sides of bar coupon for DSRW test, both sides of TiN-coated HSS coupons by Balzers were analyzed by X-ray diffraction. Figure 12 is an example of X-ray diffraction diagram from bar coupon #H7. A higher TiN peak than that of α-Fe in one side indicates a thicker coating and lower TiN peak than that of α-Fe in the other side means thinner coating. Except for one coupon (#H9), which had approximately same thicknesses in both sides, all the rest of four bars from Balzers were found to have different thicknesses on each side, based on XRD results.

Residual Stress

The free standing films from Balzers without substrates appeared concave when viewed from substrate side. This was an indication of tensile stress. However, the films from Multi-Arc showed the opposite result, i.e., compressive stress.

Surface Roughness

Table V. lists the result of surface roughness measurement on the bar coupons. Two batches of commercial high speed steel were used as the substrate materials coated with titanium nitride by Balzers and Multi-Arc respectively. Before deposition, the roughness values of the substrate which was later coated by Balzers were higher (Ra=0.57, Rmax=4.3) than those by Multi-Arc (Ra=0.41, Rmax=3.2). After deposition, their roughness values showed little change (Ra=0.56, Rmax=4.4 for the substrate coated by Balzers and Ra=0.43, Rmax=3.6 for the one coated by Multi-Arc).

3.3 Dry Sand Rubber Wheel Testing

3.3.1 Apparatus Calibration

Before DSRW tests on coatings, three samples made of mild A588 steel were tested following ASTM procedure B (2000 rev.). The coefficient of variation (ν) was 3.27% which was acceptable ($< 5\%$) according to ASTM standards. During the wear testing, five samples made of mild steel A588 were

tested following ASTM procedure C (100 rev.). The coefficient of variation (ν) was 1.88% which was also acceptable ($< 5\%$).

The DSRW test results of the coatings are composed of two parts: weight loss versus path length plot indicating the ranking of coating wear resistance and SEM photos showing coating deterioration phenomena during the wear process.

3.3.2 Weight Loss vs Path Length

Weight loss vs path length for less than 300 ft of path length is shown in Figure 13. TiN-coated HSS samples by Balzers were divided into two groups: thin TiN-coated ($\simeq 0.5\mu m$) and thick TiN-coated ($\simeq 2.0\mu m$). It is seen within this range that the thick TiN-coated HSS from Balzers had the highest wear resistance while the thin TiN-coated HSS from Balzers, thin TiN-coated HSS from Multi-Arc, and Cr-coated 1095 had the second highest wear resistance, the TiN-coated O1 tool steel had the lowest wear resistance.

Results for the total path length of 1000 ft are shown in Figure 14. The thick TiN-coated HSS from Balzers exhibited the highest wear resistance, thin TiN-coated HSS from Balzers and TiN-coated HSS from Multi-Arc had the second highest wear resistance, the Cr-coated 1095 from Precision Tool the next highest, and the TiN-coated O1 from Multi-Arc had the lowest wear resistance. Thick TiN-coated HSS from Balzers, TiN-coated O1 from Multi-Arc and Cr-coated 1095 from Precision Tool showed transition points (change of slope) in

the plot while others did not.

3.3.3 Coating Degradation Development

Cr-coated 1095 by Precision Tool

Figures 15(a) and (b) show the Cr coating surface before and after 8 ft path length of wear testing. The surface has a nodular appearance with cracks distributed all over it before testing. The top portions of those nodules on the coating surface were removed after 8 ft path length of wear process [Figure 15(b)]. The coating surfaces after 14 ft, 49 ft and 235 ft path length of wear testing are shown in Figure 16. Surface cracks distributed over the coating surface before testing [Fig. 15(a)] did not show any propagation. The coating was completely removed from its substrate at about 235 ft path length [Fig. 16(c)].

TiN-coated HSS by Multi-Arc

Many macroparticles, 4μm to 10μm in diameter, were observed dispersed on the surface of the TiN-coated HSS by Multi-Arc [Fig. 17(a)]. After 9 ft path length of wear testing, microcracks perpendicular to the direction of abrasive flow (from left to right in all the following SEM photos) can be seen on the coating surface [Fig. 17(b)]. Many areas of coating were removed from the substrate after 12 ft path length [white in Fig. 18(a)], and more coating was removed after 47 ft path length [Fig. 18(c)]. High magnification photos show microcracks on the areas of coating [Fig. 18(b)] and fragmentation of those

microcracked areas [Fig. 18(d)]. The majority of the coating was removed after a 63 ft path length (Figure 19).

TiN-coated O1 by Multi-Arc

The wear characteristics of a TiN-coated O1 tool steel by Multi-Arc were similar to those for the HSS substrate coated with TiN by Multi-Arc.

Thick TiN-coated HSS by Balzers

A small quantity of macroparticles was observed distributed on the surface of thick TiN-coated HSS by Balzers [Fig. 20(b)]. Some white spots can be seen on the coating surface after 7 ft path length of wear testing [Fig. 20(c)]. A high magnification photo of these spots shows a pit with microcracks at the leading edge where the macroparticle originally was before the test [Fig. 20(d)]. Those areas of coating removal were enlarged along the abrasive sand flow direction [Fig. 21(a)] after 73 ft path length. High magnification photos show microcracking along the edges of coating removal areas [Fig. 21(b)] and fragmentation of those microcracked areas [Fig. 21(c)]. Many areas of coating were removed after 350 ft path length of wear testing [Fig. 22(a)]. However, a majority of the coating was not removed until 583 ft path length [Fig. 22(c)]. Figure 22(b) show the leading end of a long groove where coating had been completely removed after 235 ft path length of wear testing. Microcracks can be seen along the edges of this groove. The areas of coating other than the groove showed a smooth appearance.

Thin TiN-coated HSS by Balzers

Figure 23(a) shows the the surface of a thin TiN-coated HSS by Balzers before wear testing. Overall, microcracks can be seen on the coating surface after 9 ft path length of wear testing [Fig. 23(b)], which are similar to the features seen on the Multi-Arc coating [Fig. 17(b)].

3.4 Wood Cutting Test

The wood cutting test results consist of two parts: data relating weight loss to path length, showing the ranking of coating wear resistance, and SEM photographs illustrating the coating degradation phenomena.

3.4.1 Weight Loss vs Cutting Path Length

A plot of weight loss vs cutting path length is shown in Figure 24. It can be seen that the ranking of wear resistance from the highest to the lowest is as follows: Cr-coated saw chain cutters made of 8660, TiN-coated by Multi-Arc, TiN-coated by Balzers, and the un-coated cutters.

3.4.2 Coating Degradation Development

The tips of the tested cutters, un-coated, Cr-coated (Omark), TiN-coated (Multi-Arc) and TiN-coated (Balzers) before wear testing are shown in Figure

25. Figure 26 displays the cutter tips after 5,000 ft of total cutting path length. The Cr-coated cutter [Fig. 26(b)] did not show any observable wear scars while the TiN-coated cutters exhibited narrow strips along the cutter edges where the coating had been completed removed [Fig. 26(c) and (d)]. Figure 27 shows the cutter tips after a total path length of 35,000 ft. The width of those strips were observed to be different for the different cutters, with the Cr-coated cutter being the narrowest [Fig. 27(b)], the TiN-coated from Multi-Arc the second in width [Fig. 27(c)] and the TiN-coated from Balzers the widest [Fig. 27(d)]. Compared with Figure 25, Figure 28 is a higher magnification photograph of cutter edges before wear testing in which machining burrs can be seen. Figure 29 shows the cutter edges after 5,000 ft of cutting path length. The burrs seen in Figure 28 had been removed. Very fine grooves can be seen on the cutter surfaces indicating material removal and abrasive flow direction (Fig. 29). Coatings were removed from the cutting edges of the TiN-coated cutters [Fig. 29(c) and (d)] while the Cr-coating still remained on the cutter edge [Fig. 29(b)] of Cr-coated cutters. Figure 30 shows the transition between coating areas and areas of coating removal after a total path length of 35,000 ft. Straight, fine grooves crossed the transition region on the Cr-coated cutters [Fig. 30(a)], while irregular areas of coating removal and sharp coating edges could be seen on the TiN-coated cutters. The cross-sections through the cutter clearance face are depicted in Figure 31, which shows a smooth profile on the Cr-coated cutter [Fig. 31(a)] and sharp edges on the TiN-coated cutters [Fig. 31(b) and (c)]. It also can be seen that the thickness of Cr coating is much greater than that of the TiN coatings.

4. DISCUSSION

4.1 Thickness Measurement

The coating thicknesses were measured by SEM with results obtained on several samples. The coating thicknesses may vary from where the sample for evaluation was removed and measurements made. The thickness measurement by SEM was not precise. The results of thickness measurements, therefore, can only be taken as being relative to each other. The coupons #H1 (HSS) and #O2 (tool steel) were sent together in the same batch to Multi-Arc for titanium nitride coating deposition. Their thicknesses, nevertheless, were different with the former [$\simeq$ 0.7 μm, Fig. 9(a)] having a thinner coating than the latter [$\simeq$ 1.4 μm, Fig. 9(b)]. These results and those presented in section 3.2 demonstrate that coating thicknesses can vary from company to company, from batch to batch, from sample to sample, and from side to side in a single sample. Some of the thickness variation of those commercial coatings can be considered as reasonable for the deposition process. As the transportation of vaporized particles is that of line-of-sight, the samples which face and are close to the source will be expected to have a greater thickness than others. This is a technical problem associated with the commercial PVD coating deposition and has not been solved thus far.

4.2 Weight Loss Measurement

The weights of both bar coupons for DSRW test and saw chain cutters for the wood cutting test were measured by a balance which has a sensitivity of 1×10^{-4} gm in a 200 gm range (used for measuring bar coupons) and 1×10^{-5} gm in a 40 gm range (used for measuring saw chain cutters). The balance can be considered reliable. However, there were some factors which had an influence on weight loss measurement. For example, it was found that a magnetic field existed in both bar coupons and saw chain cutters after coating deposition, which made the weight measurement vary with each repetition for the same sample. This might be account for the weight increase shown in Figure 13. Except for a few samples in the preliminary test (data points in the range of less than 50 ft path length), all the other samples in subsequent tests, including the wood cutting test, were demagnetized before testing. Another factor which might give rise to data scatter is possible variations in the cleaning of the specimens. The solutions normally used for ultrasonic cleaning such as BRANSON formulated cleaning concentrate for oxide removal, were found to either adhere to the specimens or they caused sample corrosion. A solution of half acetone and half alcohol was found to have the best cleaning effect. The samples after ultrasonic cleaning should be thoroughly dried by a blower for 5 minutes and left in the air for another 15 minutes. Environmental factors such as air moisture and room temperature also had an effect on weight measurement which was particularly significant for the saw chain cutters as their weight loss was very small in the first 5,000 ft path length ($\sim 10\times10^{-5}$ gm). Over-

night weight measurements were not comparable.

4.3 Wear Resistance Evaluation

DSRW Test

The weight loss of the TiN-coated HSS by Multi-Arc and thin TiN-coated HSS by Balzers followed a linear relationship with path length, Figures 13 and 14. It was known by observation of the specimen surfaces that the TiN coating from Multi-Arc was completed removed at about 63 ft path length. Thus the weight loss of the TiN-coated HSS by Multi-Arc over 100 ft path length was actually due to the wear of its HSS substrate. A similar situation was found in the thin TiN-coated HSS by Balzers. A transition period, shown by a change of slope in the weight loss vs path length curve, can be observed for the thick TiN-coated HSS by Balzers, Cr-coated 1095 by Precision Tool and TiN-coated O1 by Multi-Arc. Figure 22(c) indicates that a thick TiN coating on HSS from Balzers was removed after 583 ft path length, which corresponded to the transition period (Figure 14). The data points beyond 583 ft followed a straight line which had the same slope as the curves for TiN-coated HSS by Multi-Arc and thin TiN-coated HSS by Balzers with their coatings removed; and thus represented the HSS substrate wear. Similar cases were found with the TiN-coated O1 by Multi-Arc and Cr-coated 1095 by Precision Tool. This suggests that all wear after the transition period was due to the wear of substrates.

The TiN coating from Multi-Arc had the same magnitude of thickness ($\simeq$ 0.7 μm) and showed similar performance as that of the thin TiN coating from

Balzers (thickness $\approx$ 0.5 μm), which indicated that the thin TiN coating did not perform better than the HSS substrate. The weight loss before the transition period ($<$ 583 ft) for the thick TiN-coated HSS by Balzers represented the wear of TiN while that before transition period ($<$300 ft) for the Cr-coated 1095 was due to the wear of Cr coating. Comparison of these two periods indicated that TiN coating had a higher wear resistance than the Cr coating.

Wood Cutting Test

Figure 25 shows saw chain cutter tips with and without coatings before wear testing. After 5,000 ft path length of wood cutting test, narrow strips were formed along the edges of some cutter tips [Fig. 26 (c) and (d)]. They were further enlarged after 35,000 ft path length (Fig. 27). These strips were the areas where coatings had been removed. The greater the area, the lower the wear resistance. It can be seen based on the areas of coating removal in Figures 26 and 27 that the Cr-coated saw chain cutters had the highest wear resistance, the TiN-coated by Multi-Arc the second highest, the TiN-coated by Balzers the third highest, and the un-coated the lowest. This order of ranking was different from that of DSRW test. The TiN coatings had been removed from the cutting edge after a test interval of 5,000 ft (Figure 26). However, the thickness of the TiN coatings on the cutters was much smaller (1.3 μm $\sim$ 2.1 μm) than that of the Cr coating (9 μm). It thus can not be concluded that in general a Cr coating performs better than a TiN coating of similar thickness. To solve this either a test interval of less than 5,000 ft would have to be used or coatings would have to have the same thickness.

Thickness Effect

The DSRW test results showed that thin TiN coatings did not perform better than HSS and a hard Cr coating in terms of wear resistance. This suggests that a minimum coating thickness is required if the TiN coating is used for wear resistance applications in an abrasive environment similar to DSRW test. The thicknesses of those TiN coatings (1.3 $\sim$ 2.1 μm) were also smaller than that of Cr coating ($\simeq$ 9 μm) on saw chain cutters. It was observed in the wood cutting test that the TiN coating from Multi-Arc had a thickness of about 2 μm and a slightly higher wear resistance than that from Balzers which had a thickness of about 1.3 μm, which again, illustrated some kind of thickness effect. Hence it is strongly recommended for further tests that different types of coatings to be tested be deposited with the same magnitude of coating thickness, or a single type of coating with a range of thicknesses.

4.4 Sample Preparation for TEM

Samples were prepared for TEM examination but limited results were obtained. Details regarding the preparation procedure and problems are discussed in this section.

The solution of bromine and methanol was found to be able to etch the TiN films, although at a slower rate than the dissolution of the HSS substrates. The TiN coating from Multi-Arc was found to dissolve as soon as the substrate was dissolved, and thus was believed to be less corrosion resistant than the TiN

coating from Balzers. The specimens, which were in the form of slices, were glued with epoxy to a glass base, with the coating next to the glass. They must be checked frequently so that the coating would not be dissolved after the substrate was dissolved. Great care must be taken in handling as well, as the thin films were very brittle and easily broken. Free standing thick films and films with substrates which had been etched very thin were found to twist during the ion-milling thinning process, possibly due to residual stress redistribution under the ion-bombardment in the ion-milling process.

4.5 Coating Degradation

The wear grooves shown in the Figures 15(b), 16, 27(b), 29(b) and 30(a) suggest that the Cr coating degraded by a progressive material removal in both DSRW and wood cutting tests. These may be described as the result of grooving or abrasive wear. The observation made from this work is in agreement with those of Clayton and Scholl[99] and others[98].

In the DSRW test, the common feature of all TiN coatings was microcracking of the coating, although the extent was different between thick and thin coatings. The degradation of a thin coating started with overall microcracking in the abraded region. The fragments were finally removed from the coating surface by the flowing abrasive particles. Thick coating degradation started from the removal of macroparticles from the coating surface. These areas of macroparticle removal were further enlarged by a microcracking process along their edges and subsequent fragmentation of those microcracked areas. The

disadherence process in both thin and thick TiN coatings could be considered a spalling process which occurred both within the coating and at the coating/substrate interface. Spalling, therefore, can be considered the dominate wear characteristic. However, the smooth appearance on the coating surface where no macroparticle [Figure 22(b)] was present indicates that a micropolishing process partially accounted for the coating deterioration.

No microcracking was observed in the coating areas which remained on saw chain cutter edges [Figures 29(c) and (d), 30(b) and (c)] in a wood cutting test. Instead, observation suggested that the TiN coatings deteriorated by a disadherence process at the coating/substrate interface. In addition to the thickness effect discussed before, the high shear force acting in the vicinity of saw chain cutter tips[99], substrate softening after TiN coating deposition (shown in Table IV), and the higher hardness of alumina abrasives (HV 2000, the same as TiN) are considered as factors responsible for the wear behavior of TiN coatings during wood cutting test. Different substrate materials and abrasives were used in the two wear tests, with the HSS and silica abrasive in the DSRW test, and the 8660 steel and alumina abrasive in the wood cutting test. The TiN coatings at the cutter edge had been removed after a test interval of 5,000 ft while apparent Cr coating removal (strips) was observed at the cutter edge after 35,000 ft. More extensive work is therefore needed before any conclusion can be made. For further wood cutting tests, a silica abrasive, and a shorter test interval of less than 5,000 ft, are recommended.

4.6 Stoichiometry, Phase Constituents and Surface Texture

Results of XPS for coating composition, X-ray diffraction analysis regarding to coating phase constituents and surface texture, are discussed in this section.

The intensity peak area ratio of Ti/N was 4.17 for the thin TiN coating from Balzers, 3.97 for the thick TiN coating from Balzers and 3.70 for the coating from Multi-Arc. The result indicated that the ratio of Ti/N was slightly higher for the TiN coating from Balzers than the one from Multi-Arc. It is recommended that further Auger work be performed for a quantitative result.

Both types of titanium nitride coatings were consisted of single phase TiN (Figure 11). Preferred orientations are generally observed in ceramic films, such as 111, 200 and 220[24-26,34,73,81,101,102]. In the present experiment, strong 111 orientations were found in both types of TiN coatings by X-ray diffraction (Figure 12). The result was in agreement with the majority of observations according to a comprehensive review by Sundgren[73].

4.7 Residual Stress

Compressive stresses were often reported in ceramic thin films[25,51,58,64,103]. It was found that a tensile stress existed in the TiN coating from Balzers (both thin and thick), and compressive stress in the TiN coating from Multi-Arc. TiN has a thermal expansion coefficient of $9.35\times10^{-6}K^{-1}$ while that of HSS is about 13. Compressive thermal stresses, hence, would be

expected in both kinds of coatings when the coated HSS substrates were cooled down from the deposition temperature to room temperature. As no detailed information about the deposition process was provided, it is not known how the tensile stress in the coating from Balzers was developed.

4.8 Macroparticles

Macroparticles have been reported on the evaporated TiN coatings and have been found to be very detrimental to the coated tool life[21,31,48,85]. Coatings deposited by a modified evaporation process, where little or no macroparticles were present, showed a great reduction of wear compared with those coatings prepared by an unmodified evaporation process[31,48]. However, no report has been published about how these particles influence the coating deterioration. In the present work, macroparticles were observed on the TiN coatings from both Multi-Arc [Figure 17(a)] and Balzers [Figure 20(b)]. They were found to initiate the coating removal in the thick TiN coating from Balzers [Figure 20(c) and (d), and 21(a)]. No effect of these particles on coating degradation was observed in the thin TiN coatings from both companies, possibly because the coating was removed so quickly.

4.9 Deposition Techniques

No significant difference in microstructures, chemistry, and wear performance, other than thickness, was found between an arc-evaporated TiN coating (Multi-Arc) and an electron-beam evaporated TiN coating (Balzers). It is

recommended that thick TiN coatings with same thickness deposited by both processes, be evaluated in further wear tests. TEM work for coating grain size, defect distribution and density which may influence coating hardness, Auger work on coating stoichiometry, microhardness testing, and Scratch testing for coating adhesion evaluation are also suggested.

5. CONCLUSIONS

1. The thicknesses of commercial TiN coatings were not consistent from company to company, batch to batch, sample to sample and side to side in one sample.
2. A thick TiN coating had better wear resistance than an electroplated hard Cr coating in the DSRW test.
3. Thin TiN coatings did not have better wear resistance than the electroplated hard Cr coating in the DSRW test.
4. There was no difference in terms of coating deterioration between an arc evaporated TiN coating with thickness about 0.7 μm and a 0.5 μm electron beam evaporated TiN coating in the DSRW test.
5. TiN coatings degraded predominately by a spalling process while the Cr coating deteriorated by uniform grooving wear in the wear tests performed.
6. A Cr-coated saw chain cutter with 9 μm coating thickness showed better performance in terms of wear resistance than the TiN-coated cutters after 5,000 ft of wood cut.
7. Both types of TiN coatings on HSS coupons in the DSRW test were consisted of a single TiN phase and had a strong 111 surface orientation.
8. A compressive stress was found in the TiN coating on HSS by Multi-Arc and a tensile stress in the coating on HSS by Balzers.

References

1. Editorial, "Strong growth predicted for several ceramic markets," *American Ceramic Society Bulletin*, vol. 67, p. 1888, ACerS, 1988.
2. Editor, "Slow growth for ceramics," *Advanced Materials & Processes*, pp. 29-44, Jan 1989.
3. H. Randhawa, "Hard coatings for decorative applications," *Surface and Coating Technology*, vol. 36, pp. 631-646, 1988.
4. B. F. Coll and P. Jacquot, "Surface modification of medical implants and surgical devices using TiN layers," *Surface and Coating Technology*, vol. 36, pp. 867-878, 1988.
5. N. Kumar, K. Pourrezaei, M. Fissel, and T. Begley, "Growth and properties of radio frequency reactive sputtered titanium nitride thin films," *J. Vac. Sci. Technol.*, vol. A 5 (4), pp. 1778-1782, Jul/Aug 1987.
6. B. Lee, E. C. Douglas, K. Pourrezaei, and N. Kumar, "Effect of oxygen on the diffusion barrier properties of TiN," *V-MIC Conf.*, pp. 344-350, IEEE, 1987.
7. M. Wittmer, B. Studer, and H. Melchior, "Electrical characteristics of TiN contacts to N silicon," *J. Appl. Phys.*, vol. 52, no. 9, pp. 5722-5726, Sep 1981.
8. M.-A. Nicolet, "Diffusion barriers in thin films," *Thin Solid Films*, vol. 52, p. 415, 1978.
9. Rao R. Tummala, "Ceramics in microelectronic packaging," *American Ceramic Society Bulletin*, vol. 67, no. 4, pp. 752-758, ACerS, 1988.
10. H. A. Sundquist, E. H. Sirvio, and M. T. Kurkinen, "Wear of metal working tools ion plated with titanium nitride," *Metals Technology*, vol. 10, pp. 130-134, Apr 1983.
11. John B. Wachtman and L. M. Sheppard, "Inorganic thin films: Expanding Applications," *American Ceramic Society Bulletin*, vol. 68, no. 1, pp. 91-95, 1989.
12. A. Matthews, "Titanium nitride PVD coating technology," *Surface Engineering*, vol. 1 (2), pp. 93-104, 1985.
13. ASM, in *Metals Handbook Ninth Edition*, vol. 5, American Society for Metals, Metals Park, Ohio, 1980.
14. I. A. Bucklow, "Physical vapour deposition techniques," *Surfacing Journal*, pp. 3-9, Oct 1977.
15. R. F. Bunshah, "Physical vapor deposition of metals, alloys and ceramics," *New Trends in Materials Processing*, pp. 201-269, 1974.
16. R. L. Boxman and S. Goldsmith, "Cathode-spot arc coatings: physics, deposition and heating rates, and some examples," *Surface and Coatings Technol.*, vol. 33, pp. 153-167, 1987.
17. J. A. Thornton, "Recent advances in sputter deposition," *Surface Engineering*, vol. 2 (4), pp. 283-292, 1986.

18. C. V. Deshpandey and R. F. Bunshah, "Activated reactive evaporation-A review," in *Physics and Chemistry of Protective Coatings*, ed. W. D. Sproul, J. E. Greene and J. A. Thornton, AIP Conf. Proc. 149, pp. 33-48, American Institute of Physics, New York, 1986.

19. A. Matthews, "Developments in ionization assisted processes," *J. Vac. Sci. Technol.*, vol. A 3 (6), pp. 2354-2363, Nov/Dec 1985.

20. P. J. Martin, D. R. Mckenzie, R. P. Netterfield, P. Swift, S. W. Filipczuk, K. K. Muller, C. G. Pacey, and B. James, "Characteristics of titanium arc evaporation processes," *Thin Solid Films*, vol. 153, pp. 91-102, 1987.

21. H. Randawa and P. C. Johnson, "Cathodic arc deposition advances coating technology," *Research & Development*, pp. 173-184, Feb 1987.

22. Hideo Yoshihara and Hidefumi Mori, "Enhanced ARE apparatus and TiN synthesis," *J. Vac. Sci. Technol.*, vol. 16 (4), pp. 1007-1012, Jul/Aug 1979.

23. G. Dearnaley, "Developments in ion-assisted coatings," *Surface and Coatings Technol.*, vol. 33, pp. 453-467, 1987.

24. B. O. Johansson, J.-E. Sundgren, J. E. Greene, A. Rockett, and S. A. Barnett, "Growth and properties of single crystal TiN films deposited by reactive magnetron sputtering," *J. Vac. Sci. Technol.*, vol. A 3, pp. 303-307, Mar/Apr 1985.

25. K.-H. Habig, "Chemical vapor deposition and physical vapor deposition coatings: Properties, tribological behavior, and applications," *J. Vac. Sci. Technol.*, vol. A 4 (6), Nov/Dec 1986.

26. J.-E. Sundgren, B.-O. Johansson, S.-E. Karlsson, and H. T. G. Hentzell, "Mechanisms of reactive sputtering of titanium nitride and titanium carbide II: Morphology and structure," *Thin Solid Films*, vol. 105, pp. 367-384, 1983.

27. J.-E. Sundgren, B.-O. Johansson, H. T. G. Hentzell, and S.-E. Karlsson, "Mechanisms of reactive sputtering of titanium nitride and titanium carbide I: Influence of process parameters on film composition," *Thin Solid Films*, vol. 105, pp. 353-366, 1983.

28. J.-E. Sundgren, B.-O. Johansson, H. T. G. Hentzell, and S.-E. Karlsson, "Mechanisms of reactive sputtering of titanium nitride and titanium carbide III: Influence of substrate bias on composition and structure," *Thin Solid Films*, vol. 105, pp. 385-393, 1983.

29. D. S. Rickerby and P. J. Burnett, "Correlation of process and system parameters with structure/and properties of physically vapor deposit hard coatings," *Thin Solid Films*, vol. 157, pp. 195-222, 1988.

30. Pengxing Li, M. Zhang, X. Qi, X. Lin, and F. Yang, "The structures and interfaces of TiN films prepared by hollow cathode discharge ion plating technique," *J. Vac. Sci. Technol.*, vol. A 5 (2), pp. 187-190, Mar/Apr 1987.

31. S. Boelens and H. Veltrop, "Hard coatings of TiN, (TiHf) and (TiNb)N deposited by random and steered arc evaporation," *Surface and Coatings Technol.*, vol. 33, pp. 63-71, 1987.

32. B. E. Jacobson, R. Nimmagadda, and R. F. Bunshah, "Microstructures of TiN and Ti2N deposits prepared by activated reactive evaporation," *Thin Solid Films*, vol. 63, pp. 333-339, 1979.

33. M. K. Hibbs, B. O. Johansson, J.-E. Sundgren, and U. Helmersson, "Effects of substrate temperature and substrate material on the structure of reactively sputtered TiN films," *Thin Solid Films*, vol. 122, pp. 115-129, 1984.

34. O. A. Johansen, J. H. Dontje, and R. L. D. Zenner, "Reactive arc vapor ion deposition of TiN, ZrN and HfN," *Thin Solid Films*, vol. 153, pp. 75-82, 1987.

35. R. Manory, "Effects of deposition parameters on structure and composition of reactively sputtered TiNx films," *Surface Engineering*, vol. 3 (3), pp. 233-238, 1987.

36. A. J. Perry, L. Simmen, and L. Chollet, "Ion-plated HfN coatings," *Thin Solid Films*, vol. 118, pp. 271-277, 1984.

37. U. Helmersson, H. T. G. Hentzell, L. Hultman, M. K. Hibbs, and J.-E. Sundgren, "Growth, structure and properties of TiN coating on steel substrates," in *Physics and Chemistry of Protective Coatings*, ed. W. D. Sproul, J. E. Greene and J. A. Thornton, AIP Conf. Proc. 149, pp. 79-94, New York, 1986.

38. U. Helmersson, J.-E. Sundgren, and J. E. Greene, "Microstructure evolution in TiN films reactively sputter deposited on multiphase substrates," *J. Vac. Sci. Technol.*, vol. A 4, p. 500, May/Jun 1986.

39. L. Hultman, H. T. G. Hentzell, J.-E. Sundgren, B.-O. Johansson, and U. Helmersson, "Initial growth of TiN on different phases of high speed steel," *Thin Solid Films*, vol. 124, pp. 163-170, 1985.

40. M. K. Hibbs, J.-E. Sundgren, B. O. Johansson, and B. E. Jacobson, "The microstructure of reactively sputtered TiN films containing the Ti2N phase," *Acta metall.*, vol. 33, pp. 797-803, 1985.

41. P. J. Martin, R. P. Netterfield, D. R. McKenzie, I. S. Falconer, C. G. Pacey, P. Tomas, and W. G. Sainty, "Characterization of a Ti vacuum arc and the structure of deposited Ti and TiN films," *J. Vac. Sci. Technol.*, vol. A 5 (1), pp. 22-28, Jan/Feb 1987.

42. L. S. Wen, X. Jiang, and C. Y. Si, "A transmission electron microscopy study on Ti-N films deposited by ion plating," *J. Vac. Sci. Technol.*, vol. A 4 (6), pp. 2682-2685, Nov/Dec 1986.

43. J. M. Molarius, A. S. Korhonen, and E. O. Ristolainen, "Ti-N phases formed by reactive ion plating," *J. Vac. Sci. Technol.*, vol. A 3 (6), pp. 2419-2425, Nov/Dec 1985.

44. D. S. Rickerby, A. M. Jones, and A. J. Perry, "Structure of titanium nitride coatings deposited by physical vapor deposition: A unified structure model," *Surface and Coating Technology*, vol. 36, pp. 631-646, 1988.

45. H. Rudigier, E. Bergmann, and J. Vogel, "Properties of ion-plated TiN coatings grown at low temperatures," *Surface and Coating Technology*, vol.

36, pp. 675-682, 1988.

46. H. M. Gabriel and K. H. Kloos, "Morphology and structure of ion-plated TiN, TiC and Ti(C,N) coatings," *Thin Solid Films*, vol. 118, pp. 243-254, 1984.
47. K. Y. Ahn, M. Wittmer, and C. Y. Ting, "Investigation of TiN films reactively sputtered using a sputter gun," *Thin Solid Films*, vol. 107, pp. 45-54, 1983.
48. H. Randhawa, "TiN-coated high speed steel cutting tools," *J. Vac. Sci. Technol.*, vol. A 4 (6), pp. 2755-2758, Nov/Dec 1986.
49. S. Vuorinen, E. Niemi, and A. S. Korhonen, "Microstructural study of TiN-coated threading taps," *J. Vac. Sci. Technol.*, vol. A 3 (6), pp. 2445-2449, Nov/Dec 1985.
50. P. J. Burnett and D. S. Rickerby, "The erosion behaviour of TiN coatings on steels," *J. Materials Science*, vol. 23, pp. 2429-2443, 1988.
51. D. S. Rickerby, "Internal stress and adherence of titanium nitride coatings," *J. Vac. Sci. Technol.*, vol. A 4 (6), pp. 2809-2814, Nov/Dec 1986.
52. E. Erturk and H.-J. Heuvel, "Adhesion and structure of TiN arc coatings," *Thin Solid Films*, vol. 153, pp. 135-147, 1987.
53. U. Helmersson, B. O. Johansson, and J.-E. Sundgren, "Adhesion of titanium nitride coatings on high-speed steels," *J. Vac. Sci. Technol.*, vol. A 3, pp. 308-315, Mar/Apr 1985.
54. M. Y. Al-jaroudi, H. G. T. Hentzell, and J. Valli, "The influence of the TiN deposition temperature on the critical load and hardness of hardened steels," *Thin Solid Films*, vol. 154, pp. 425-429, 1987.
55. B. E. Jacobson, C. V. Deshpandey, H. J. Doerr, A. A. Karim, and R. F. Bunshah, "Microstructure and hardness of Ti(C,N) coatings on steel prepared by the activated reactive evaporation technique," *Thin Solid Films*, vol. 118, pp. 285-292, 1984.
56. E. A. Almond, "Aspects of various processes for coating and surface hardening," *Vacuum*, vol. 34, p. 835, 1984.
57. B. M. Kramer, "Requirements for wear-resistant coatings," *Thin Solid Films*, vol. 108, p. 117, 1983.
58. D. S. Rickerby, B. A. Bellamy, and A. M. Jones, "Internal stress and microstructure of titanium coatings," *Surface Engineering*, vol. 3 (2), pp. 138-146, 1987.
59. R. Y. Fillit and A. J. Perry, "Residual stress and X-ray elastic constants in highly textured physically vapor deposited coatings," *Surface and Coating Technology*, vol. 36, pp. 647-659, 1988.
60. A. J. Perry and L. Chollet, "States of residual stress both in films and in their substrates," *J. Vac. Sci. Technol.*, vol. A 3 (6), pp. 2801-2808, Nov/Dec 1986.

61. L. Chollet and A. J. Perry, "The stress in ion-plated HfN and TiN coatings," *Thin Solid Films*, vol. 123, pp. 223-234, 1985.

62. T. Hirsch and P. Mayr, "Residual stresses and residual stress distributions in TiCN- and TiN-coated steels," *Surface and Coating Technology*, vol. 36, pp. 729-741, 1988.

63. I. Yoshizawa, Z. Kabeya, and K. Kamada, "Residual stress in coated low-z films of TiC and TiN: II. Correlation of residual stress with microstructure," *J. of Nuclear Materials*, vol. 122 & 123, pp. 1315-1319, 1984.

64. J.-E. Sundgren and H. T. G. Hentzell, "A review of the present state of art in hard coatings grown from the vapor phase," *J. Vac. Sci. Technol.*, vol. A 4 (5), pp. 2259-2279, Sep/Oct 1986.

65. R. W. Hoffman, in *Physics of Thin Films*, ed. R. E. Thun, vol. 3, p. 211, Academic, New York, 1966.

66. J. A. Thornton and D. W. Hoffman, "The influence of discharge current on the intrinsic stress in Mo films deposited using cylindrical and planar magnetron sputtering sources," *J. Vac. Sci. Technol.*, vol. A 3 (3), pp. 576-, 1985.

67. A. Pan and J. E. Greene, "Interfacial chemistry effects on the adhesion of sputter-deposited TiC films to steel substrates," *Thin Solid Films*, vol. 97, p. 79, 1982.

68. R. L. Hatschek, "Coatings: revolutions in HSS tools," *American Machinist Special Rep.*, vol. 752, p. 128, Mar 1983.

69. E. Valkonen, T. Karlsson, and B.-O. Johansson, in *Thin Film Technologies*, p. 401, 1983.

70. B. Karlsson, J.-E. Sundgren, and B.-O. Johansson, "Optical constants and spectral selectivity of titanium carbonitrides," *Thin Solid Films*, vol. 87, p. 181, 1982.

71. M. K. Hibbs, J.-E. Sundgren, B. E. Jacobson, and B.-O. Johansson, "The microstructure of reactively sputtered Ti-N films," *Thin Solid Films*, vol. 107, pp. 149-157, 1983.

72. in *Metals Handbook Eighth Edition*, ed. T. Lyman, vol. 8, p. 322,369, ASM, Metals Park, Ohio, 1973.

73. J.-E. Sundgren, "Structure and properties of TiN coatings," *Thin Solid Films*, vol. 128, pp. 21-44, 1985.

74. L. E. Toth, *Transition metal carbides and nitrides*, p. 87, Academic Press, New York, 1971.

75. J.-E. Sundgren, B. O. Johansson, A. Rockett, S. A. Barnett, and J. E. Greene, "TiNx($0.6<x<1.2$): Atomic arrangements, electronic structure, and recent recent results on crystal growth and physical properties of epitaxial layers," in *Physics and Chemistry of Protective Coatings*, ed. J. A. Thornton, AIP Conf. Proc. 149, pp. 116-129, American Institute of Physics, New York, 1986.

76. MCIC, "NITRIDES/Ti, Zr, Hf," in *Handbook No.7, Engineering Property Data on Selected Ceramics*, MCIC Rep., vol. 1, p. 5.3.4, 5.3.12, Metals and Ceramic Information Center, 1979.

77. A. K. Chattopadhyay and A. B. Chattopadhyay, "Wear and performance of coated carbide and ceramic tools," *Wear*, vol. 80, pp. 239-258, 1982.

78. C. T. Young, P. C. Becker, and S. K. Rhee, *Performance evaluation of TiN and TiC/TiN coated drills*, pp. 235-242.

79. T. Roth, E. Broszeit, and K. H. Kloos, "Influence of elastohydrodynamic conditions in highly loaded lubricated contacts on the wear behavior of TiN coatings prepared by R. F. bias sputtering," *Surface and Coating Technology*, vol. 36, pp. 765-772, 1988.

80. H. Holleck and H. Schulz, "Preparation and behavior of wear-resistant TiC/TiB2, TiN/Tib2 and TiC/TiN coatings with high amounts of phase boundaries," *Surface and Coating Technology*, vol. 36, pp. 701-714, 1988.

81. J. C. Knight, *The effect of annealing on the hardness, interfacial adhesion and wear behaviour of PVD TiN-coated steels*, 2, pp. 575-583, ASTM, New York, Apr 1989.

82. O. Knotek, R. Elsing, M. Atzor, and H.-G. Prengel, *The influence of the composition and coating parameters of PVD TiAlV(C,N) films on abrasive and adhesive wear of coated cemented carbides*, 2, pp. 557-561, ASTM, New York, Apr 1989.

83. E. Bergmann, J. Vogel, and L. Simmen, "Failure mode analysis of coated tools," *Thin Solid Films*, vol. 153, pp. 219-231, 1987.

84. W. D. Sproul, "Wear of sputter deposited refractory-metal nitride coatings," in *Physics and Chemistry of Protective Coatings*, ed. W. D. Sproul, E J. E. Greene and E J. A. Thornton, AIP Conf. Proc. 149, pp. 157-172, American Institute of Physics, New York, 1986.

85. P. Clayton and M. Scholl, "Wear of titanium nitride coatings," in *Proc. 2nd Int. Conf. on Surface Engineering*, p. Paper 4, Stratford-upon-Avon UK, 16-18 June 1987.

86. B. H. El-Bialy, A. H. Redford, and B. Mills, "Proposed wear mechanism for titanium nitride coated high speed steel," *Surface Engineering*, vol. 2 (1), pp. 29-34, 1986.

87. S. Osenius, A. S. Korhonen, and M. S. Sulonen, "Performance of TiN-coated tools in wood cutting," *Surface land Coatings Technol.*, vol. 33, pp. 141-151, 1987.

88. R. N. Bolster, I. L. Singer, R. A. Kant, B. D. Sartwell, and C. R. Gossett, "ribological behavior of TiN films deposited by high energy ion-assisted deposition ," *Surface and Coating Technology*, vol. 36, pp. 781-790, 1988.

89. S. J. Bull, D. S. Rickerby, T. Robertson, and A. Hendry, "The abrasive wear resistance of sputter ion plated titanium nitride coatings," *Surface and Coating Technology*, vol. 36, pp. 743-754, 1988.

90. A. Erdemir and R. F. Hochman, "Surface metallurgical and tribological characteristics of TiN-coated bearing steels," *Surface and Coating Technology*, vol. 36, pp. 755-763, 1988.

91. G. R. Fenske, N. Kaufherr, R. H. Lee, B. M. Kramer, R. F. Bunshah, and W. D. Sproul, "Characterization of coating wear phenomena in nitride- and carbide-coated tool inserts," *Surface and Coating Technology*, vol. 36, pp. 791-800, 1988.

92. S. Ramalingam, "Tribological characteristics of thin films and applications of thin film technology for friction and wear reduction," *Thin Solid Films*, vol. 118, pp. 335-349, 1984.

93. P. J. Burnett, "The wear and erosion resistance of hard PVD coatings," *Surface and Coating Technology*, vol. 33, pp. 191-211, 1987.

94. P. Hedenqvist, M. Olsson, and S. Soderberg, "Influence of TiN coating on wear of high speed steel tools as studied by new laboratory wear test," *Surface Engineering*, vol. 5, pp. 141-150, 1989.

95. T. S. Eyre, "Selecting the optimum surfacing technique for wear resistance," in *Proc. 2nd Int. Conf. on Surface Engineering*, p. Paper 43, Stratford-upon-Avon UK, 16-18 June 1987.

96. O. Knotek, W. D. Munz, and T. Leyendecker, "Industrial deposition of binary, ternary, and quaernary nitrides of titanium, zirconium, and aluminum," *J. Vac. Sci. Technol.*, vol. A 5 (4), pp. 2173-2179, 1987.

97. M. Scholl and P. Clayton, "Wear behavior of wood-cutting edges," *Wear*, vol. 120, pp. 221-232, 1987.

98. B. E. Klamecki, "A review of wood cutting tool wear literature," *Holzals Roh-und werkstoff*, vol. 37, pp. 265-276, 1979.

99. M. Scholl and P. Clayton, unpublished report, pp. 1-34, Mar 1987.

100. ASTM, in *1986 Annual Book of ASTM Standards*, vol. 03.02, pp. 355-373, ASTM, 1986.

101. A. Matthews and H. A. Sundquist, "Tribological Studies of Ti-N Films Formed by Reactive Ion Plating," in *Proc. of the Int. Ion Engineering Congress*, ed. Toshinori Takagi, vol. 2, pp. 1325-30, Institute of Electrical Engineers of Japan, Tokyo, Sep 1983.

102. N. Kumar, J. T. McGinn, K. Pourrezaei, B. Lee, and E. C. Douglas, "Transmission electron microscopy studies of brown and golden titanium nitride films as diffusion barries in very large scale integrated circuits," *J. Vac. Sci. Technol.*, vol. A 6 (3), pp. 1602-1608, May/Jun 1988.

103. L. Chollet, H. Boving, and H. E. Hintermann, "Residual stress measurement of refractory coatings as a nondestructive evaluation," *J. Materials for Energy Systems*, vol. 6, pp. 293-299, Mar 1985.

Table I. Mechanical and thermal properties of some typical hard coating materials and some substrate materials

Material	Young's modulus (kN/mm^{-2})	Poissons ratio	Thermal expansion coefficient ($10^{-6}K^{-1}$)	Hardness ($kg\ mm^{-2}$)	Melting or decomposition temperature (°C)
Coatings					
TiC	450	0.19	7.4	2900	3067
HfC	464	0.18	6.6	2700	3928
TaC	285	0.24	6.3	2500	3983
WC	695	0.19	4.3	2100	2776
Cr_3C_2	370	...	10.3	1300	1810
TiN	250-599	...	9.35	2000	2949
Al_2O_3	400	0.23	9.0	2000	2300
TiB_2	480	...	8.0	3370	2980
Substrates					
94WC-6Co	640	0.26	5.4	1500	...
High speed steels	250	0.30	12-15	800-1000	...
Al	70	0.35	23	30	658

Table II. Chemical composition of substrate materials (wt%)

Substrate	C	Mn	Cr	Ni	Mo	Si	P	W	V	S
HSS(DSRW)	0.89	0.49	4.39	0.79	3.06	0.46	0.05	3.87	1.40	
O1(DSRW)	0.99	1.10	0.46	0.19		0.40		0.49	0.12	
1095(DSRW)	0.97	0.39				0.25	0.02			0.034
8660(WC)	0.60	0.80	0.60	0.50	0.10	0.10				

Table II. Chemical composition of substrate materials (wt%)

Substrate	C	Mn	Cr	Ni	Mo	Si	P	W	V	S
HSS(DSRW)	0.89	0.49	4.39	0.79	3.06	0.46	0.05	3.87	1.40	
O1(DSRW)	0.99	1.10	0.46	0.19		0.40		0.49	0.12	
1095(DSRW)	0.97	0.39				0.25	0.02			0.034
8660(WC)	0.60	0.80	0.60	0.50	0.10	0.10				

Table III. Substrates and commercial coating company

Tests	Balzers(TiN)	Multi-Arc(TiN)	Precision Tool(Cr)	Omarks(Cr)
DSRW	HSS	HSS, O1	1095	
Wood cutting	8660	8660		8660

Table IV. Substrate hardnesses before and after coating

Specimens		Hardness, HRC
for DSRW test		
before coating	HSS	64.1
	O1 tool steel	60.0
	1095	64.1
after coating	HSS (coated with TiN by Multi-Arc)	63.5
	HSS (coated with TiN by Balzers)	64.4
	O1 (coated with TiN by Multi-Arc)	52.5
	1095 (coated with Cr by Precision Tool)	56.4
for wood cutting test		
before coating	8660	53.6
after coating	8660 (coated with Cr by Omark)	53.5
	8660 (coated with TiN by Multi-Arc)	51.6
	8660 (coated with TiN by Balzers)	47.6

Table V. Surface roughness

Substrate	Coating	Source	Ra ±0.06μm	Rmax(DIN) ±0.8μm
HSS	before deposition		0.41	3.2
	TiN	Multi-Arc	0.43	3.6
HSS	before deposition		0.57	4.3
	TiN	Balzers	0.56	4.4
AISI 1095	Cr	Precision Tool	0.56	4.7

Ra is the arithmetic mean of the departures of the roughness profile from the mean line. This mean line is positioned such that the area under the profile above the mean line equals to the area above the profile below the mean line.

$$Ra = \frac{1}{l_m} \int_0^{l_m} |f(x)|\, dx$$

Rmax(DIN) is the maximum peak-to-valley height of the profile in a single sampling length.

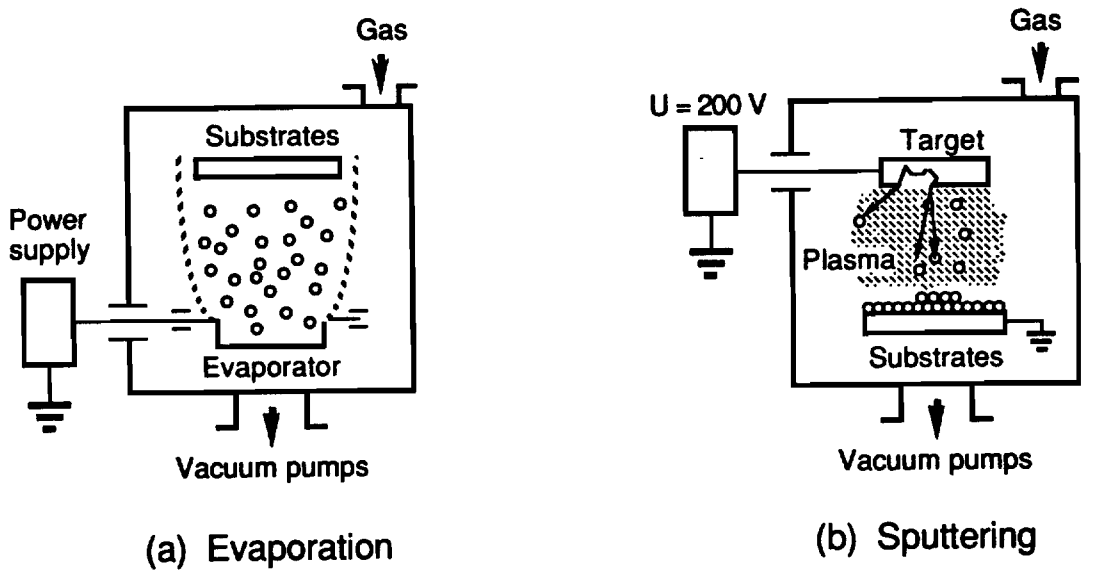

Figure 1. Basic PVD processes.

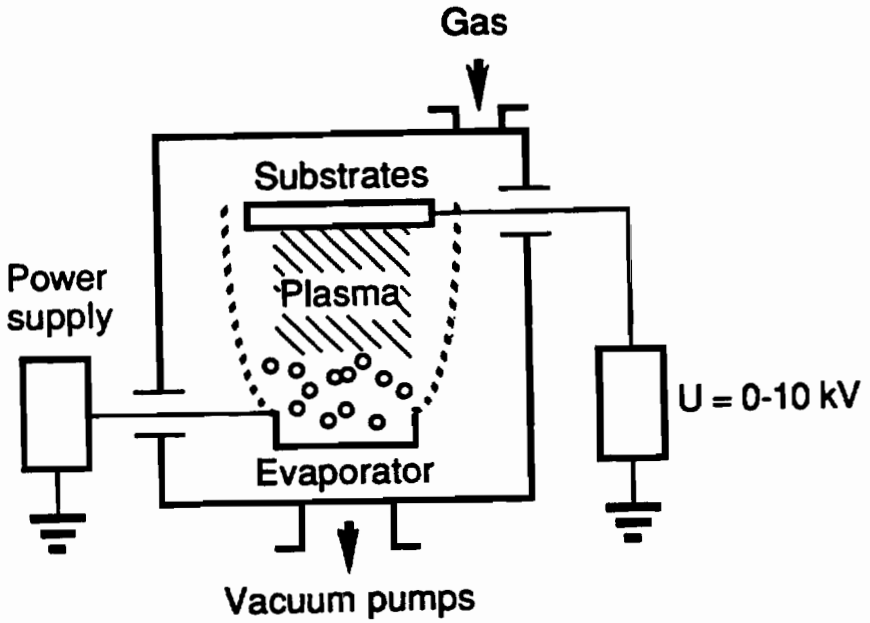

Figure 2. Ionization assisted evaporation.

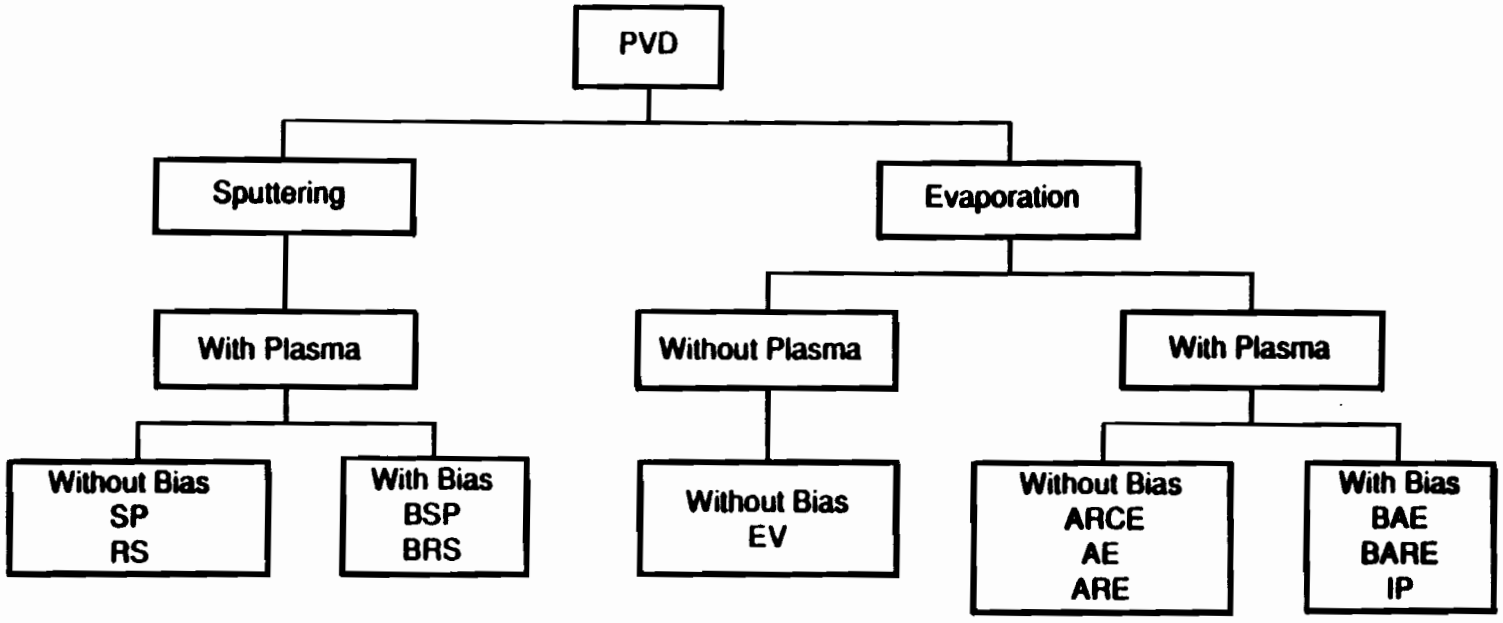

AE = activated evaporation
ARCE = arc evaporation
ARE = activated reactive evaporation
BAE = biased activated evaporation
BARE = biased activated reactive evaporation
BRS = biased reactive sputtering
BSP = biased sputtering
EV = evaporation
IP = ion plating
RS = reactive sputtering
SP = sputtering

Figure 3. Hierarchy of PVD processes.

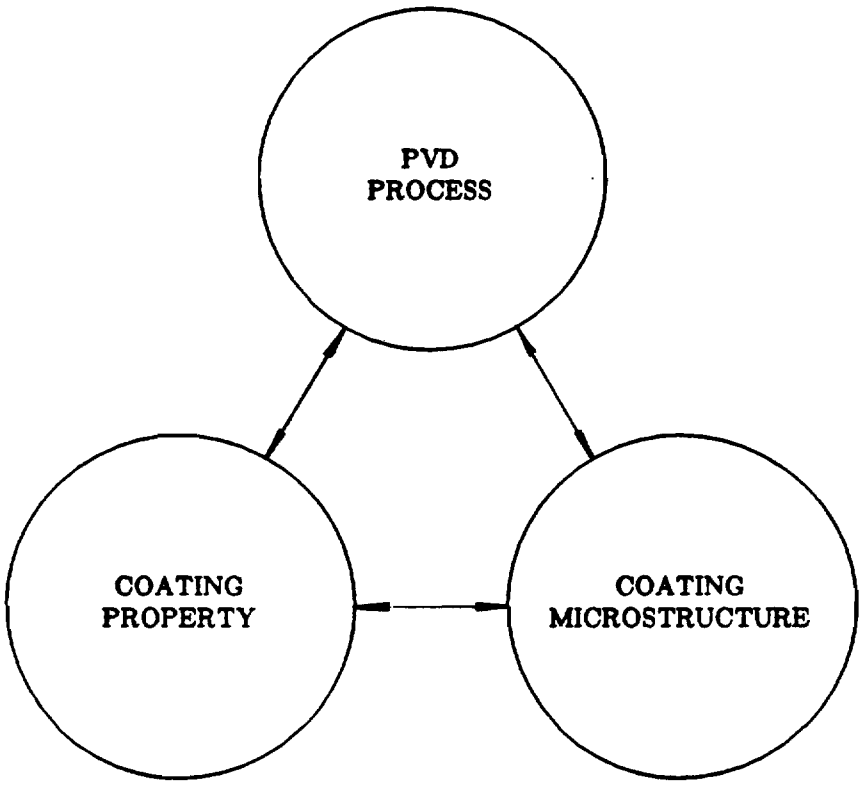

Figure 4. Research circuit in PVD technology.

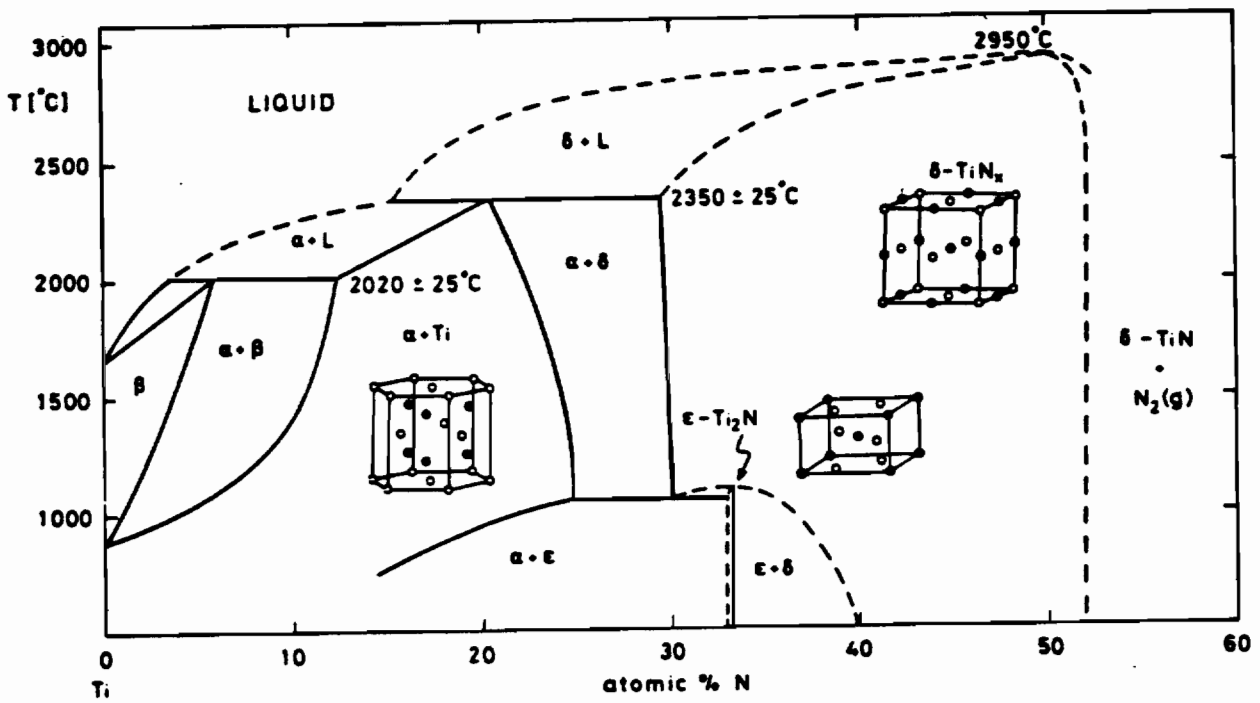

Figure 5. The Ti-N phase diagram.

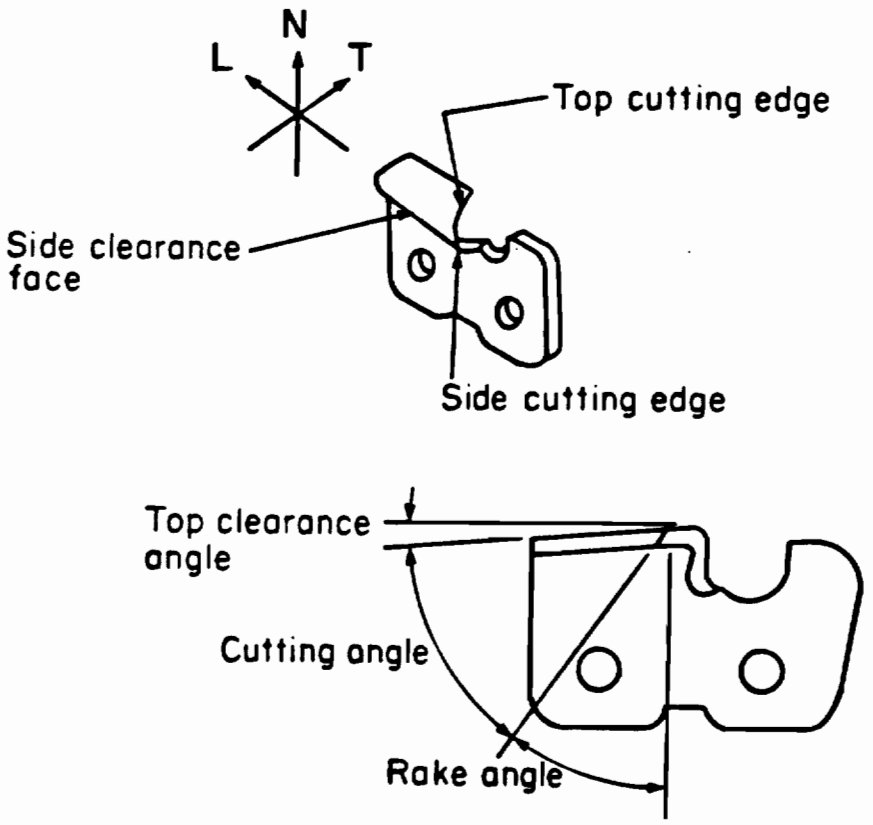

Figure 6. Diagram of saw chain cutter geometry.

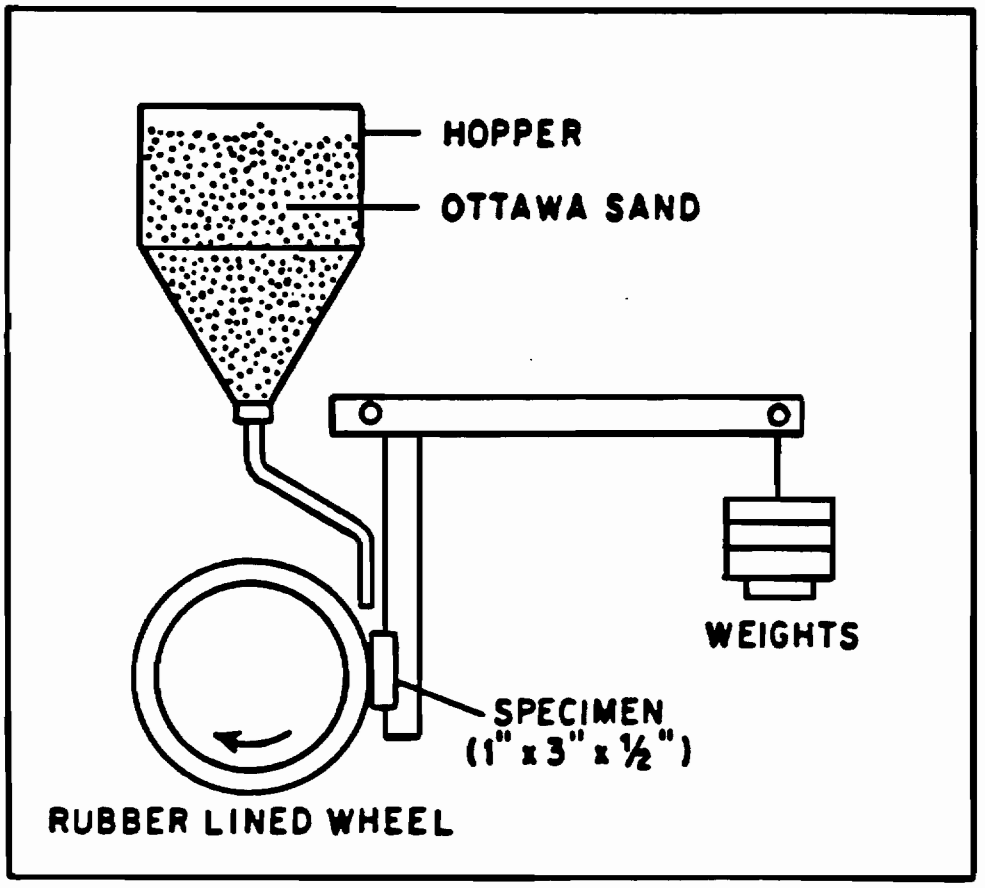

Figure 7. Schematic of Dry Sand Rubber Wheel test apparatus.

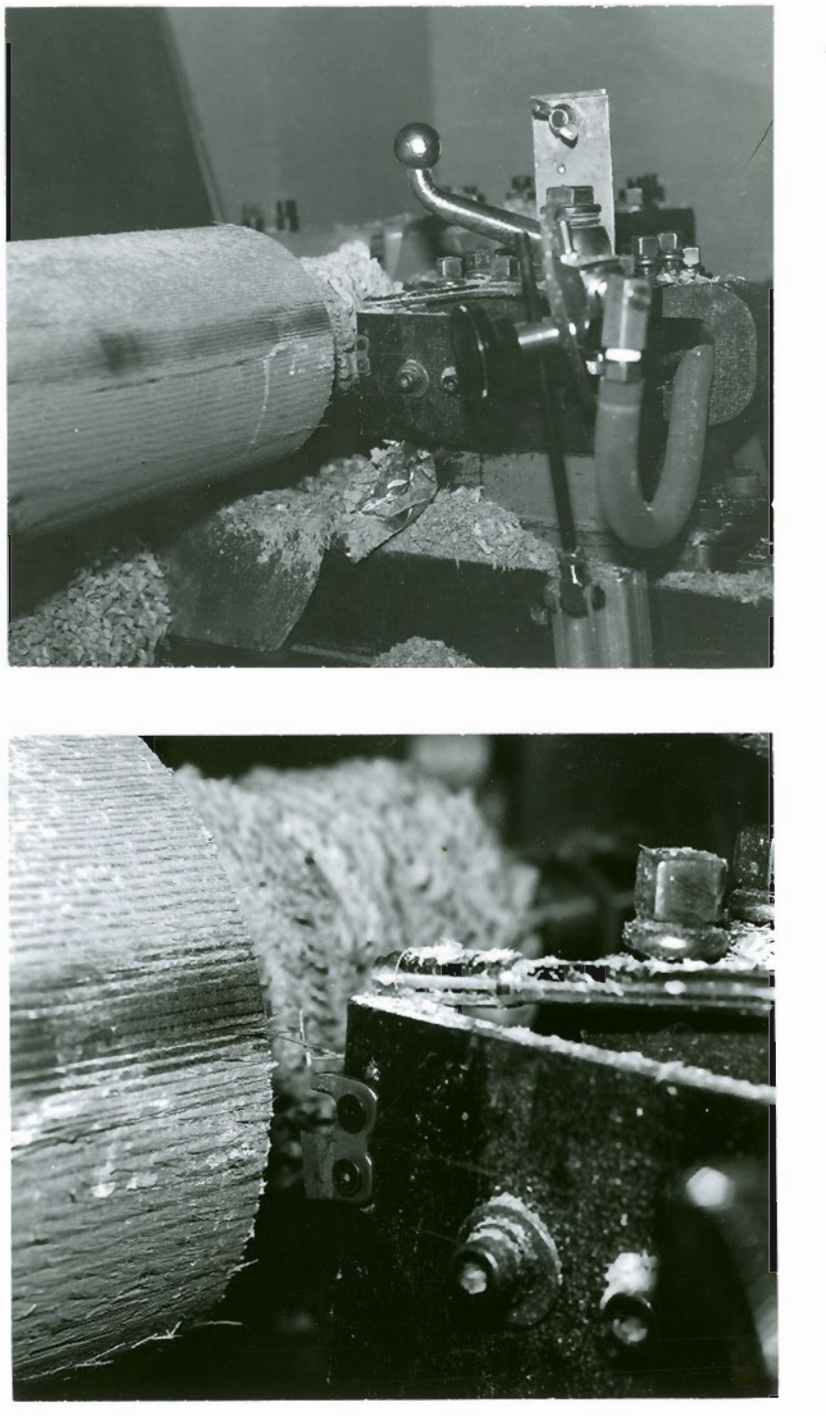

Figure 8. Wood cutting test set up showing cutter fixturing.

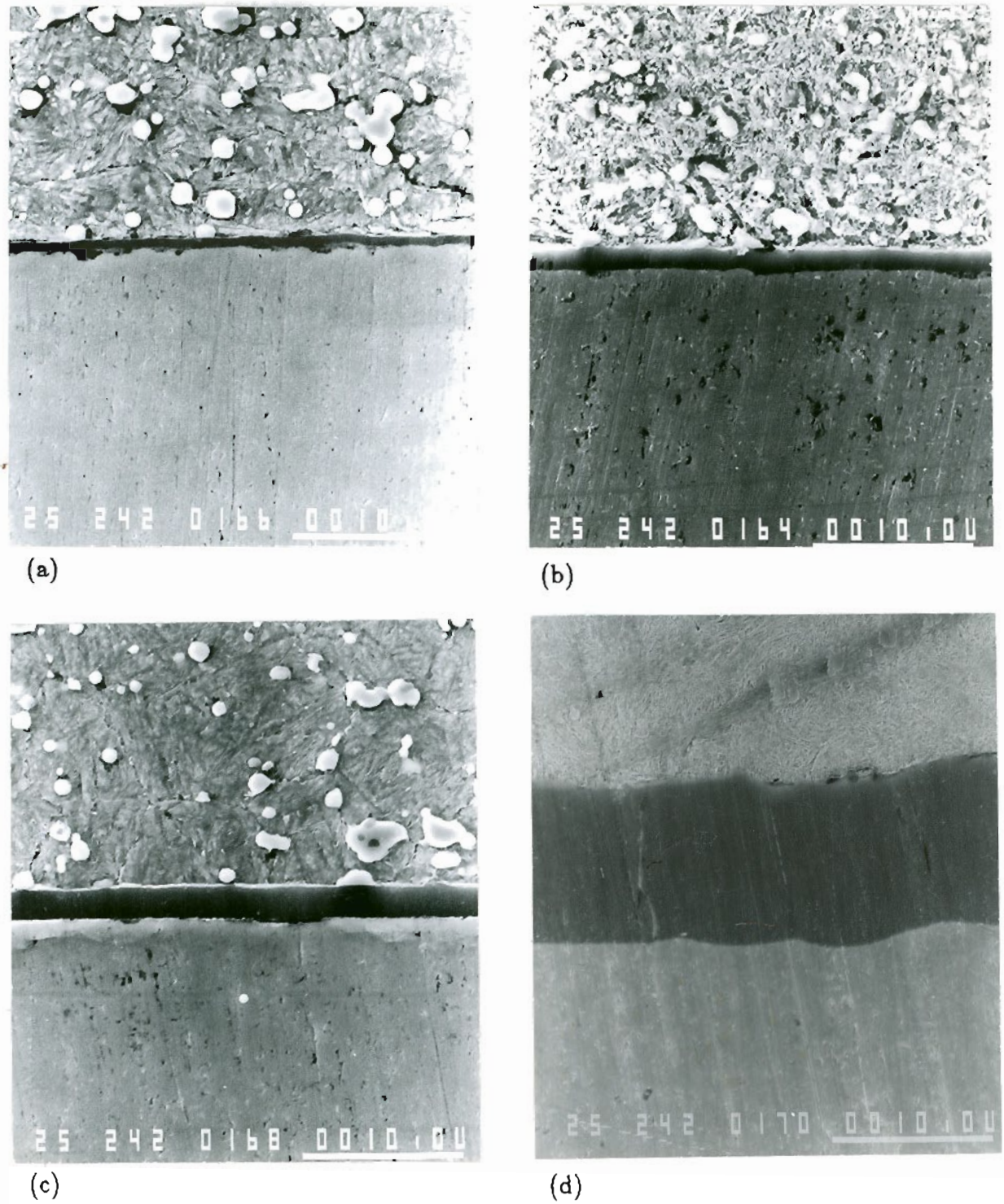

(a) (b)

(c) (d)

Figure 9. Cross-sections of (a) TiN-coated HSS by Multi-Arc, (b) TiN-coated O1 tool steel by Multi-Arc, (c) thick TiN-coated HSS by Balzers and (d) Cr-coated 1095 by Precision Tool.

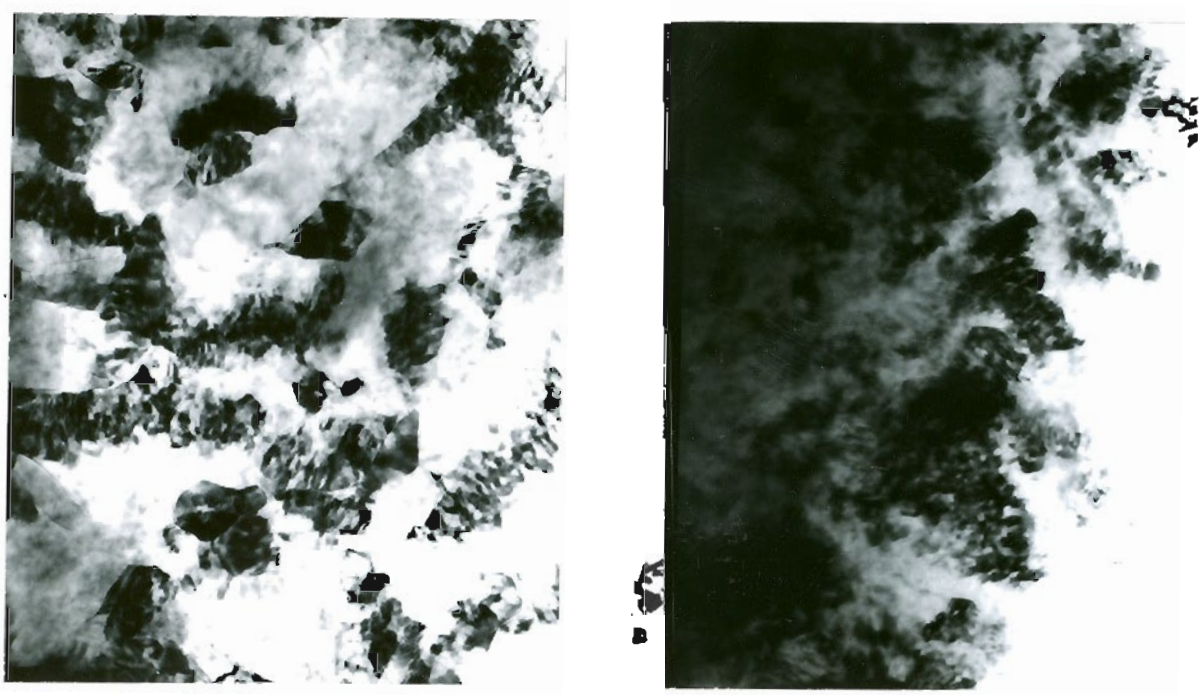

Figure 10. Transmission electron micrograph showing polycrystalline microstructures of (a) TiN coating from Balzers and (b) TiN coating from Multi-Arc.

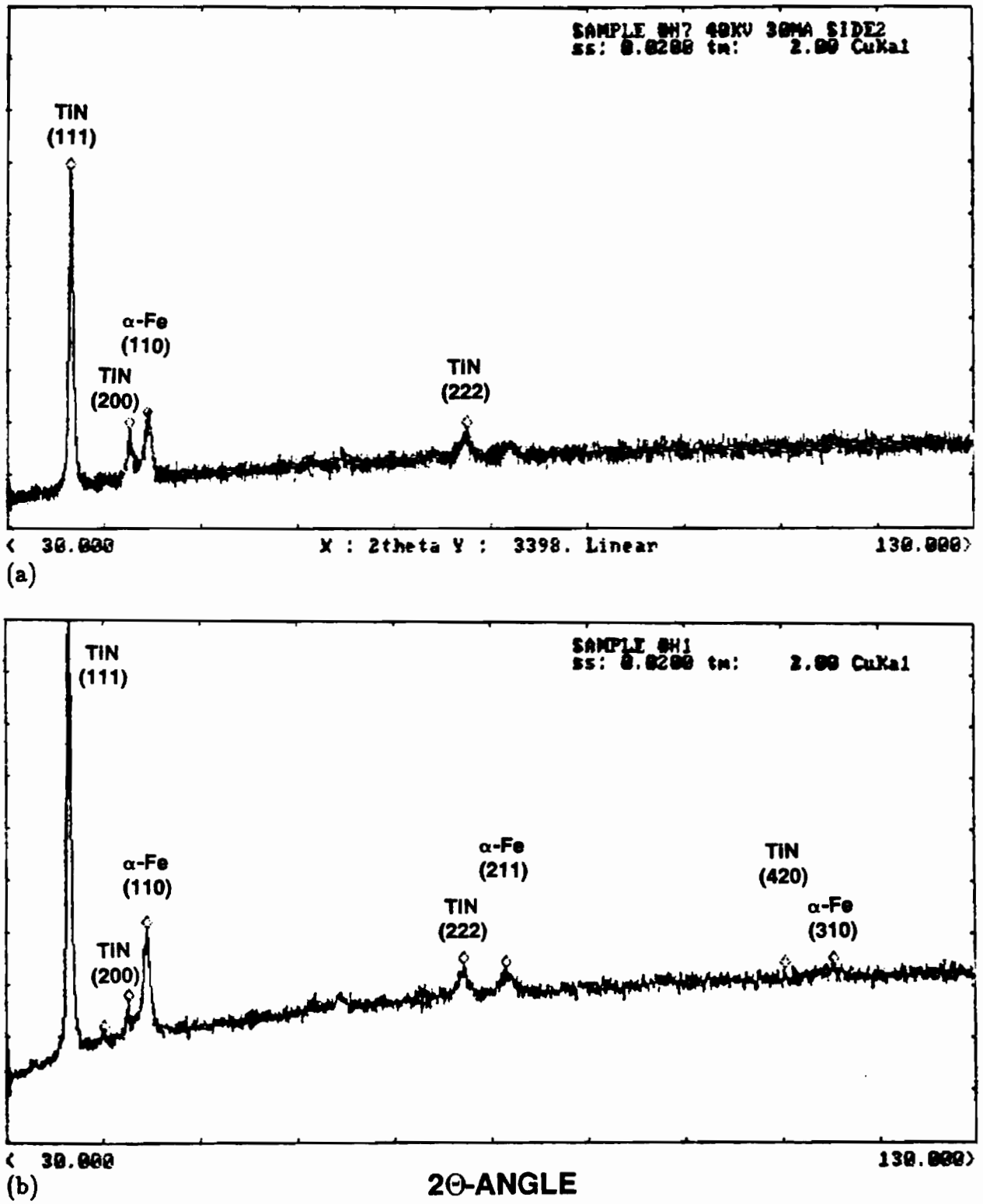

Figure 11. XRD diagrams showing single TiN phase and strong 111 orientation: (a) thick TiN coating from Balzers and (b) TiN coating from Multi-Arc.

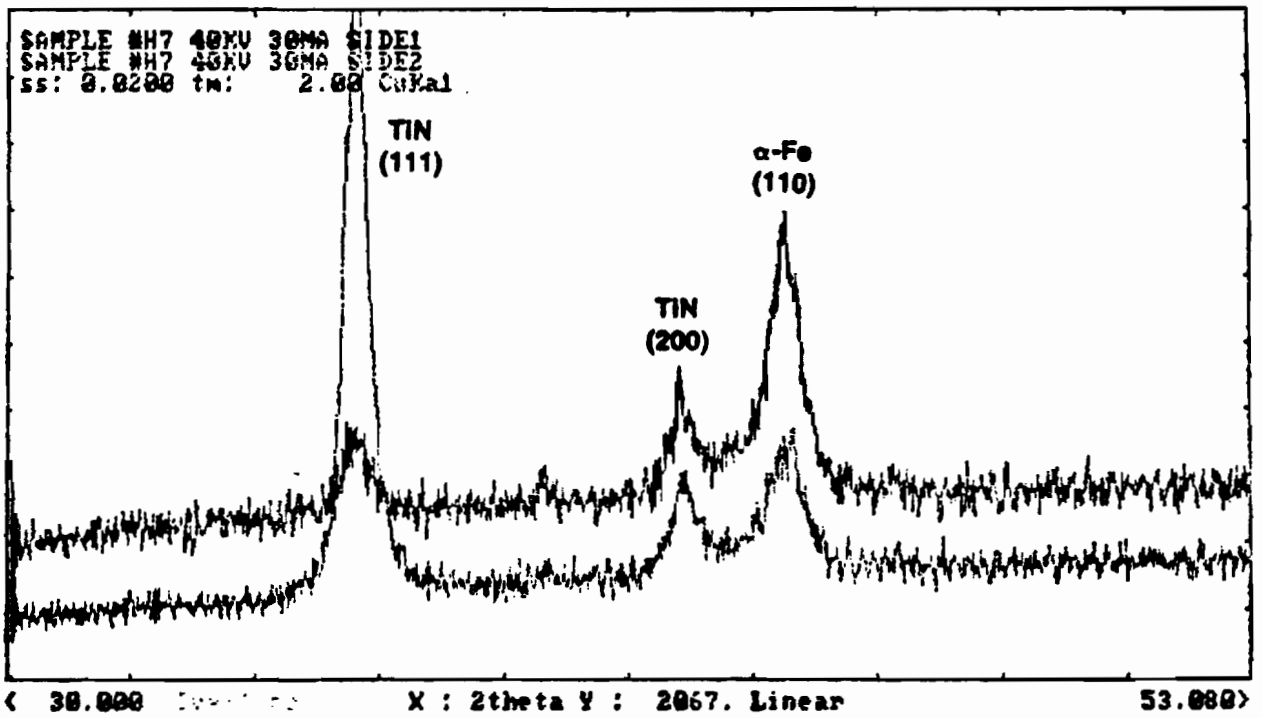

Figure 12. Superimposed XRD diagrams from the two sides of a TiN-coated HSS coupon by Balzers showing high TiN peak in one side indicating thick TiN coating, and low TiN peak in the other indicating thin TiN coating.

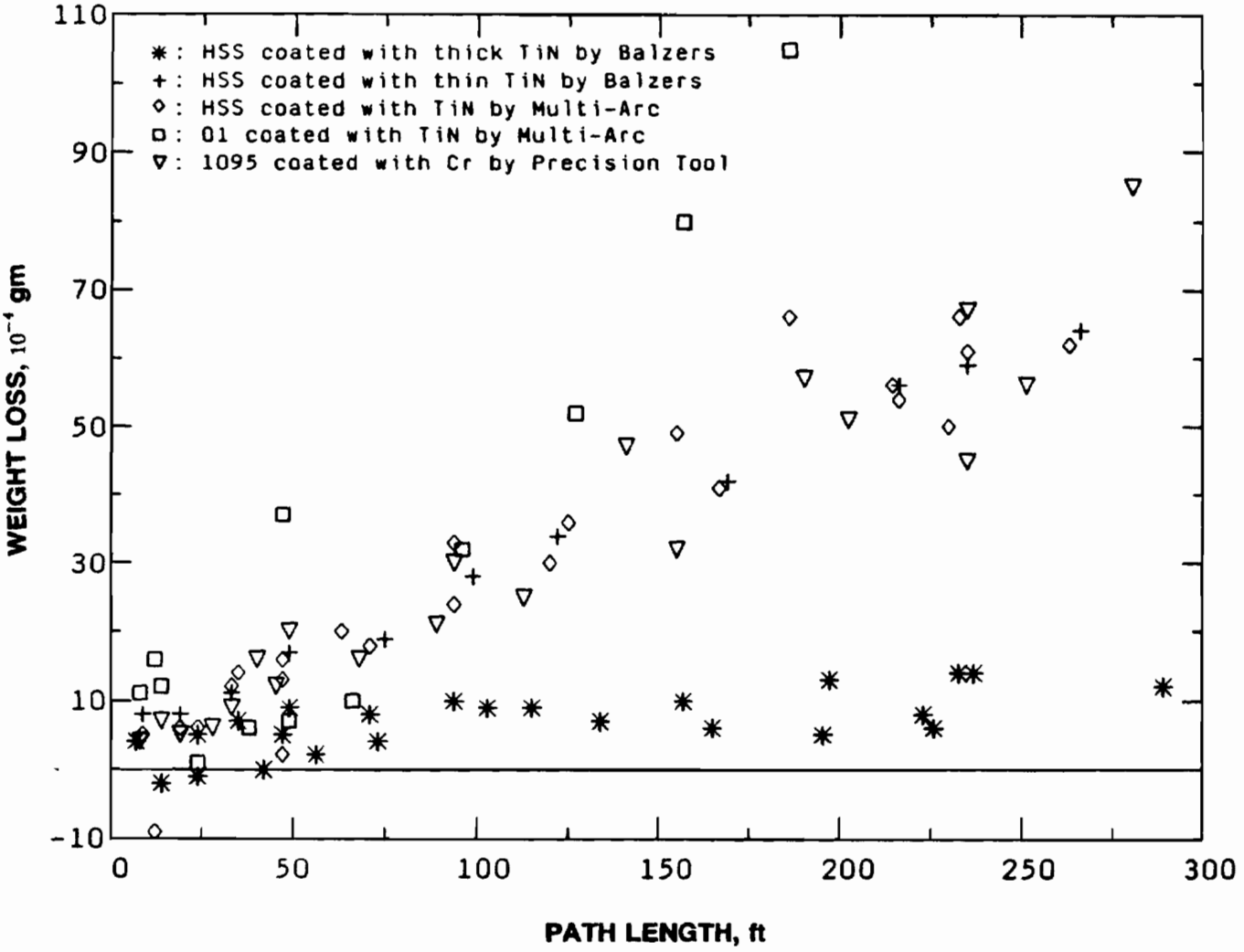

Figure 13. The result of Dry Sand Rubber Wheel (DSRW) test (total path length $<$ 300 ft).

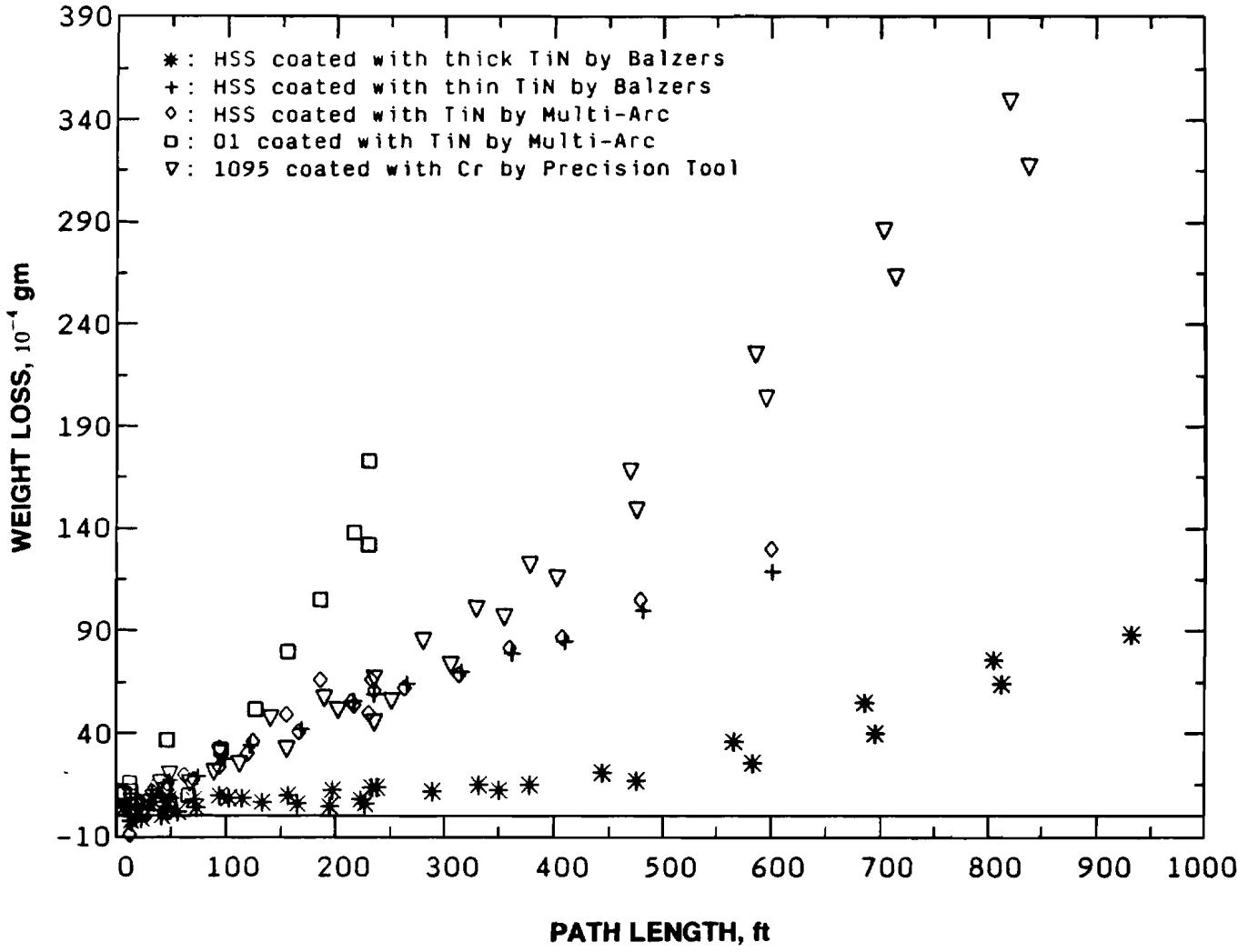

Figure 14. The result of Dry Sand Rubber Wheel (DSRW) test (total path length of 1000 ft).

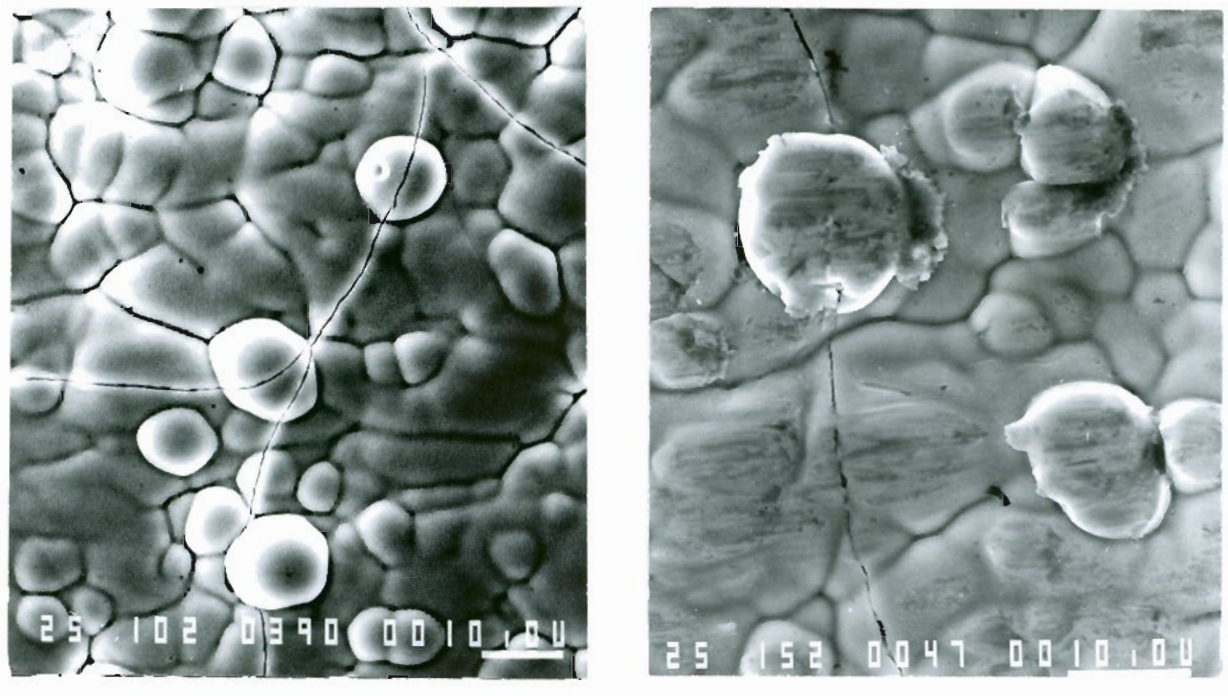

(a) (b)

Figure 15. Surface topography of Cr-coated 1095 before wear testing (a) and after 8 ft path length of DSRW testing (b).

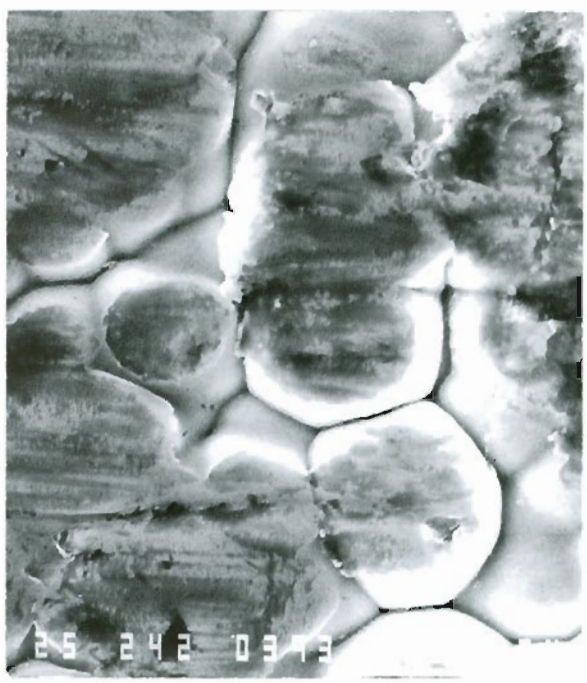

(a)

(b)

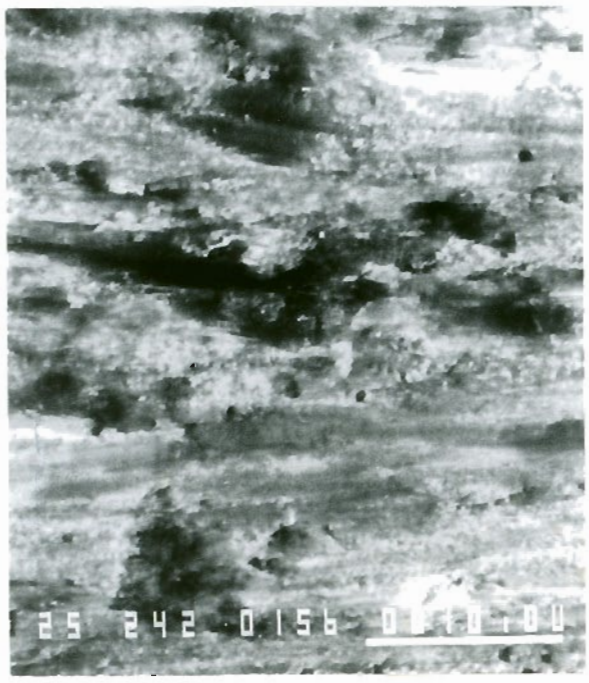

(c)

Figure 16. Surface topography of Cr-coated 1095 after (a) 14 ft, (b) 49 ft, and (c) 235 ft path length of DSRW testing.

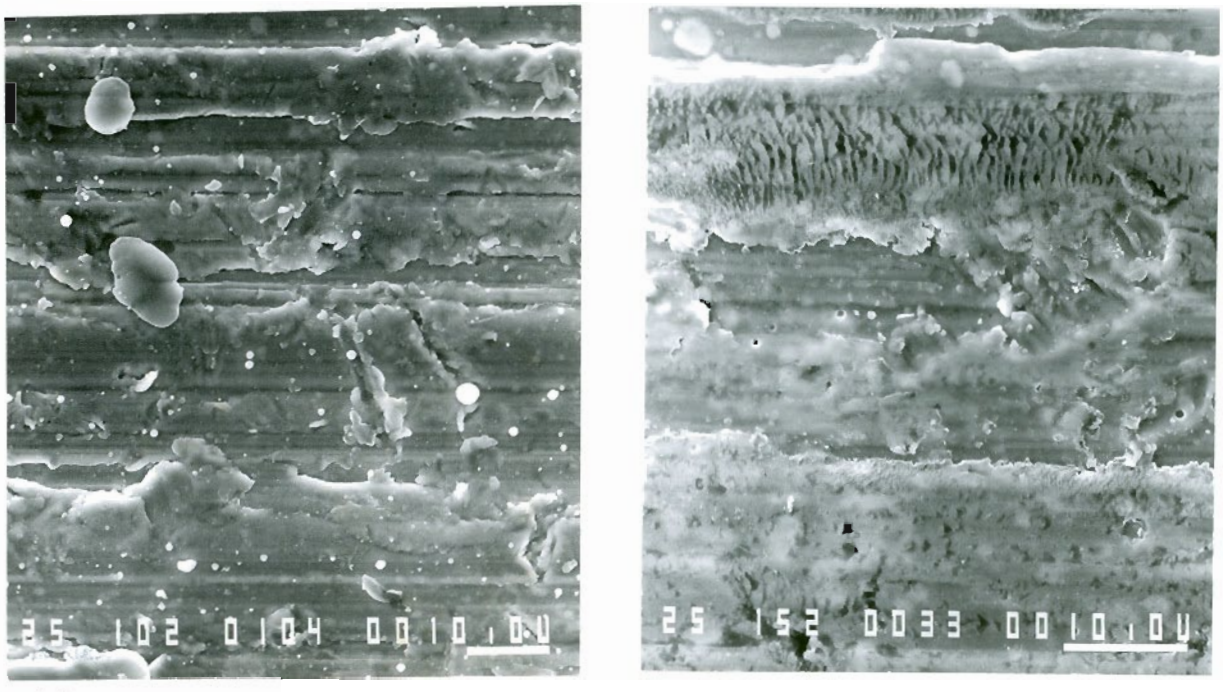

(a) (b)

Figure 17. Surface topography of TiN-coated HSS by Multi-Arc before wear testing (a) and after 9 ft path length of DSRW testing (b).

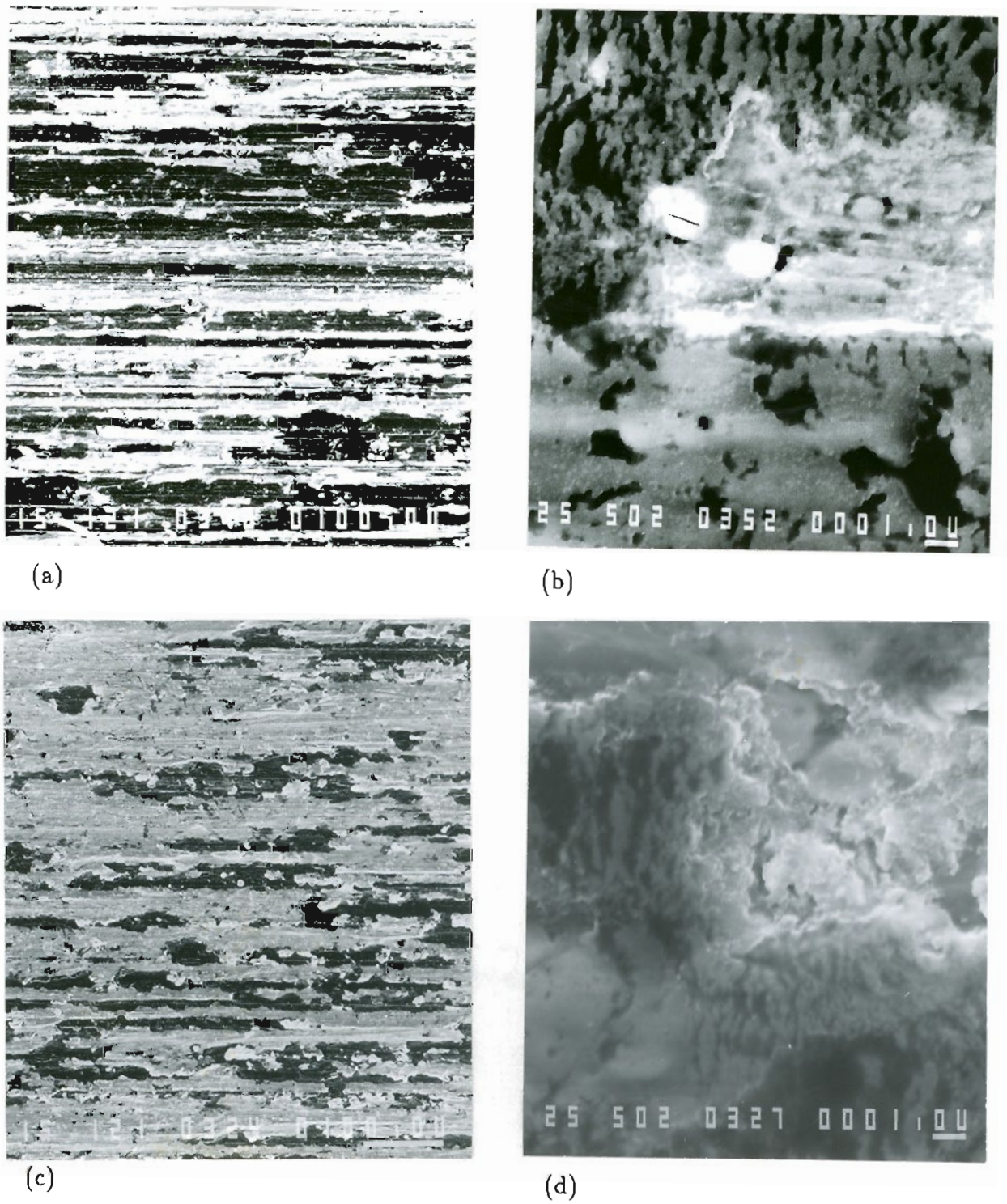

(a) (b)

(c) (d)

Figure 18. Surface topography of TiN-coated HSS by Multi-Arc after 12 ft (a and b) and 47 ft (c and d) path length of DSRW testing.

Figure 19. Surface topography of TiN-coated HSS by Multi-Arc after 63 ft path length of DSRW testing.

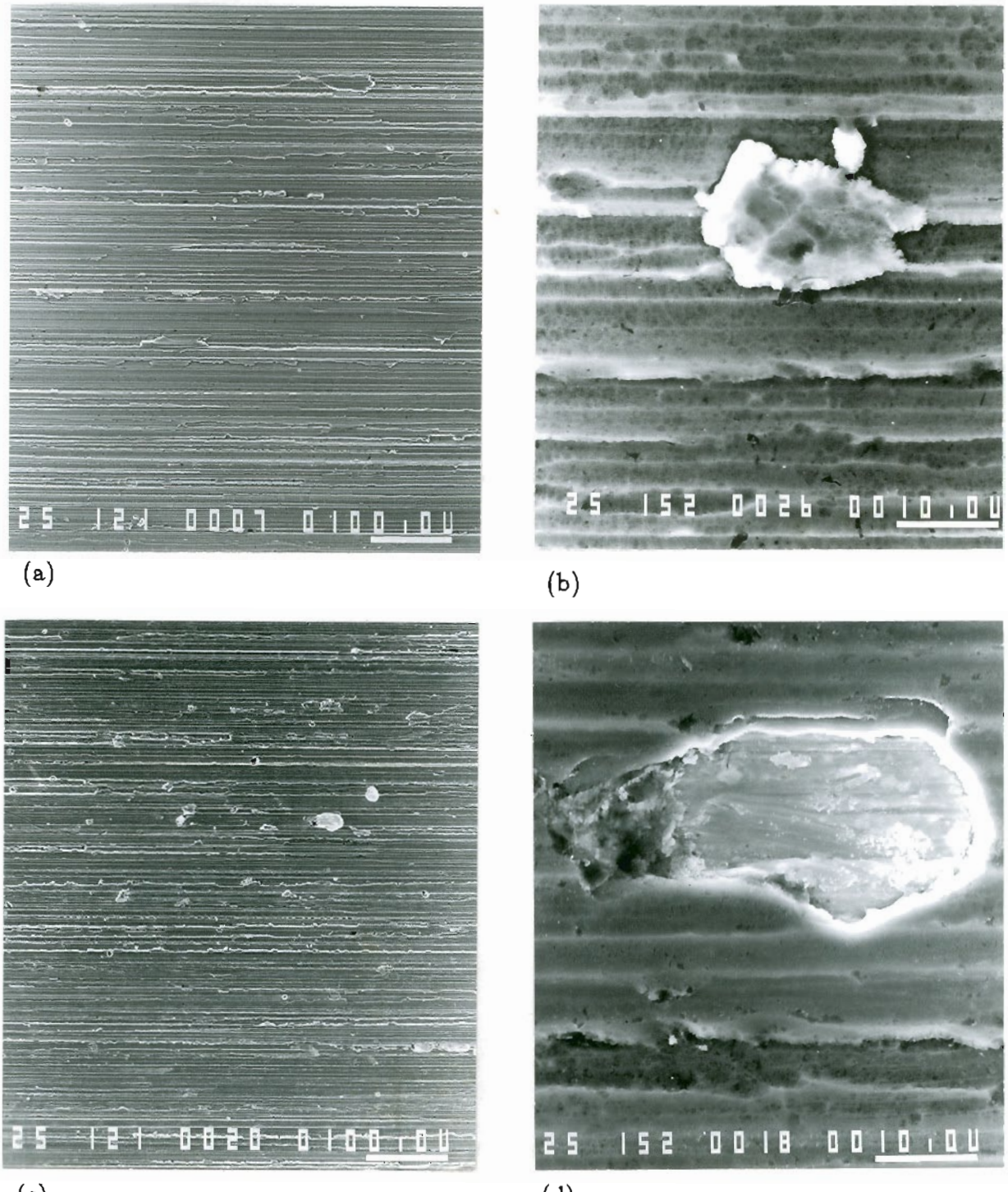

(a) (b)

(c) (d)

Figure 20. Surface topography of thick TiN-coated HSS by Balzers before wear testing (a and b), and after 7 ft path length of DSRW testing (c and d).

(a)

(b)

(c)

Figure 21. Surface topography of thick TiN-coated HSS by Balzers after 73 ft path length of DSRW testing: (a) low magnification, (b) high magnification showing microcracks in the coating areas and (c) a further higher magnification showing fragmentation of microcracked areas.

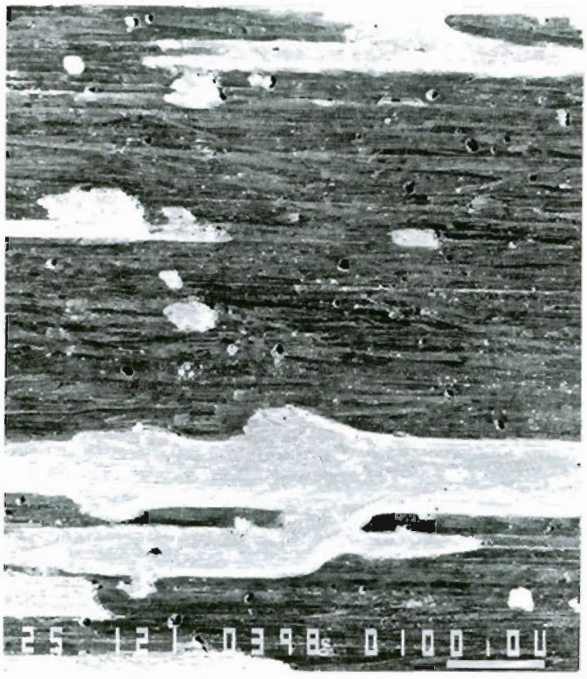

(a)

(b)

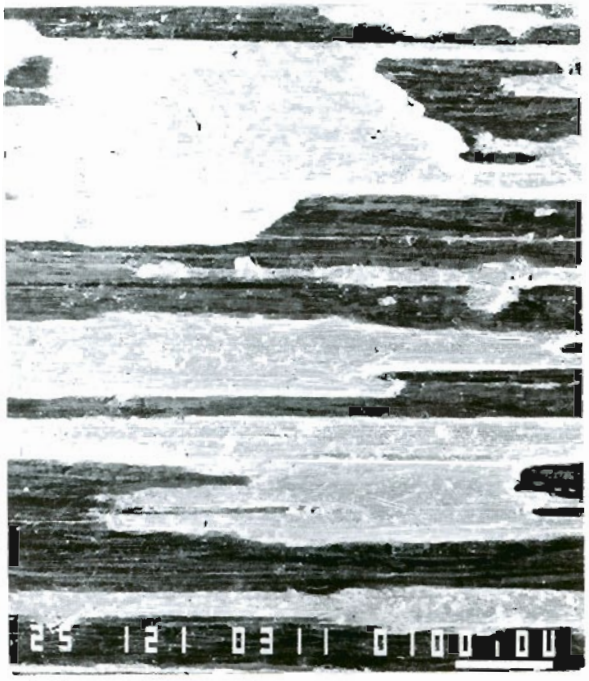

(c)

Figure 22. Surface topography of thick TiN-coated HSS by Balzers after 350 ft (a) and (b), and 583 ft (c) path length of DSRW testing.

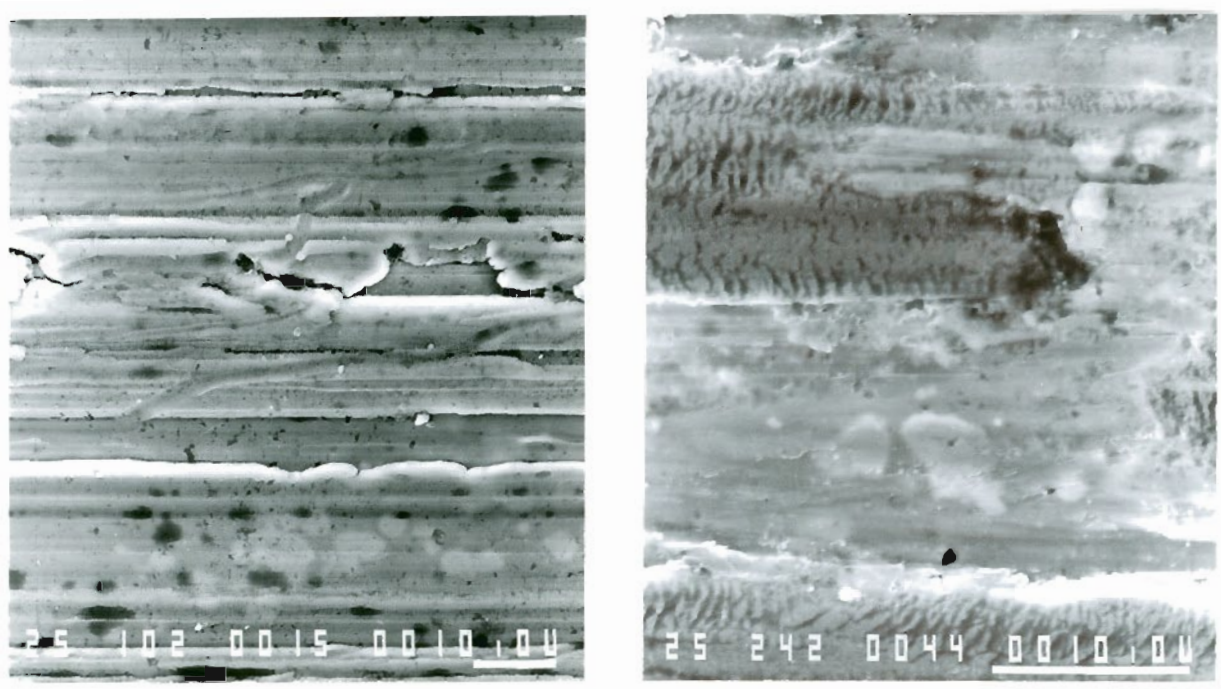

(a) (b)

Figure 23. Surface topography of thin TiN-coated HSS by Balzers before wear testing (a) and after 9 ft path length of DSRW testing (b).

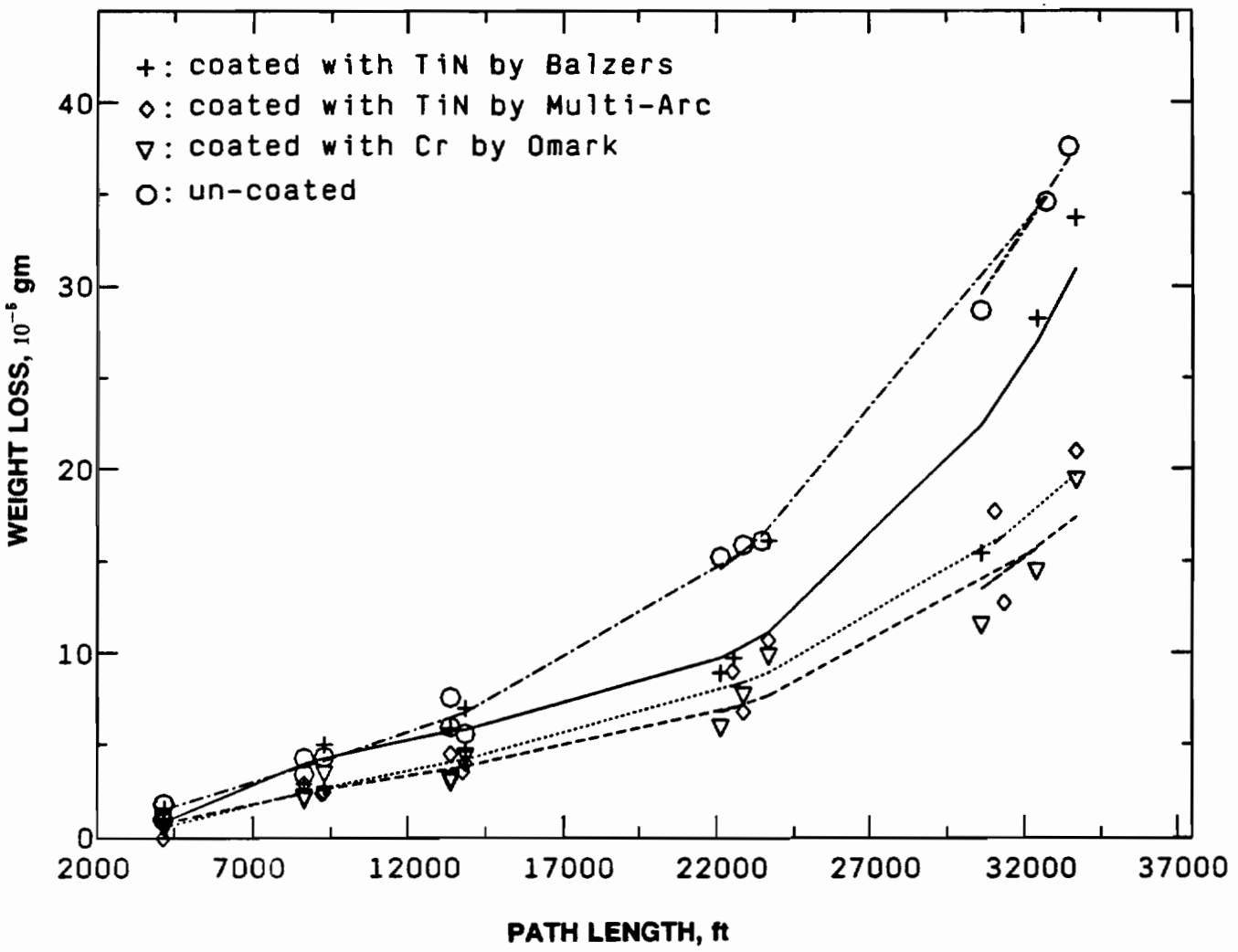

Figure 24. Result of wood cutting test.

(a)

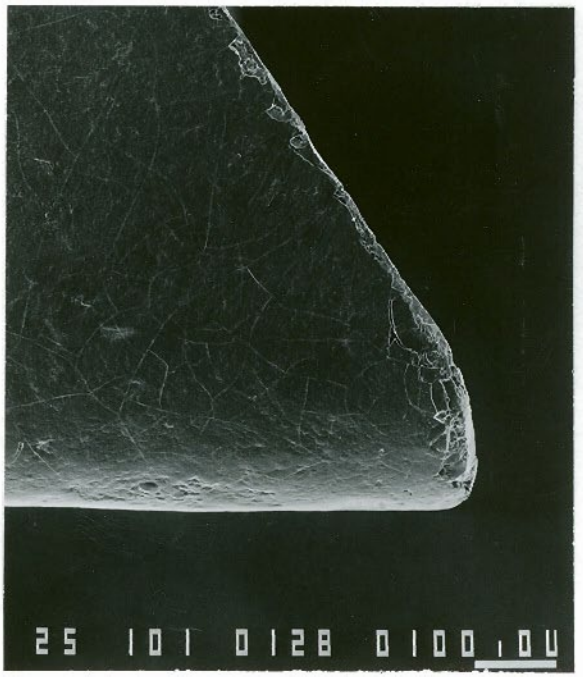

(b)

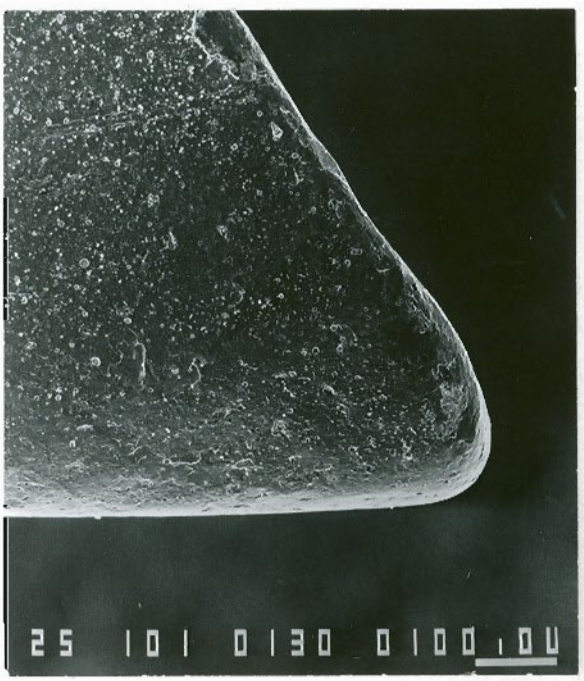

(c)

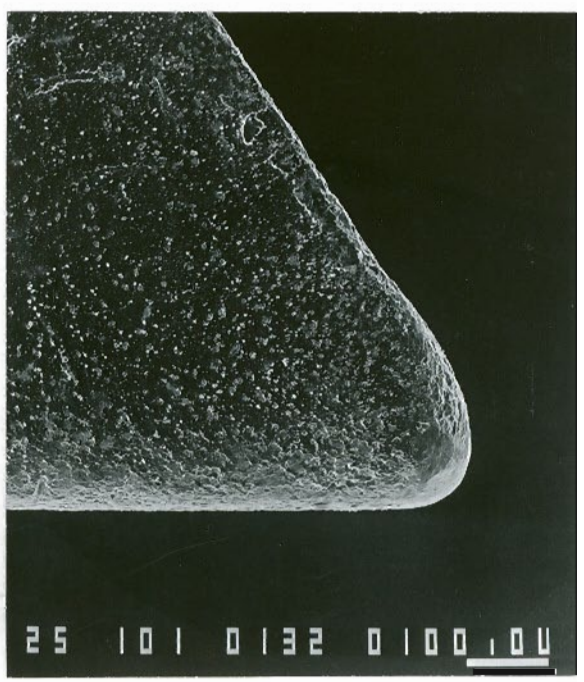

(d)

Figure 25. Saw chain cutter tips before wear testing: (a) un-coated, (b) Cr-coated by Omark, (c) TiN-coated by Multi-Arc, and (d) TiN-coated by Balzers.

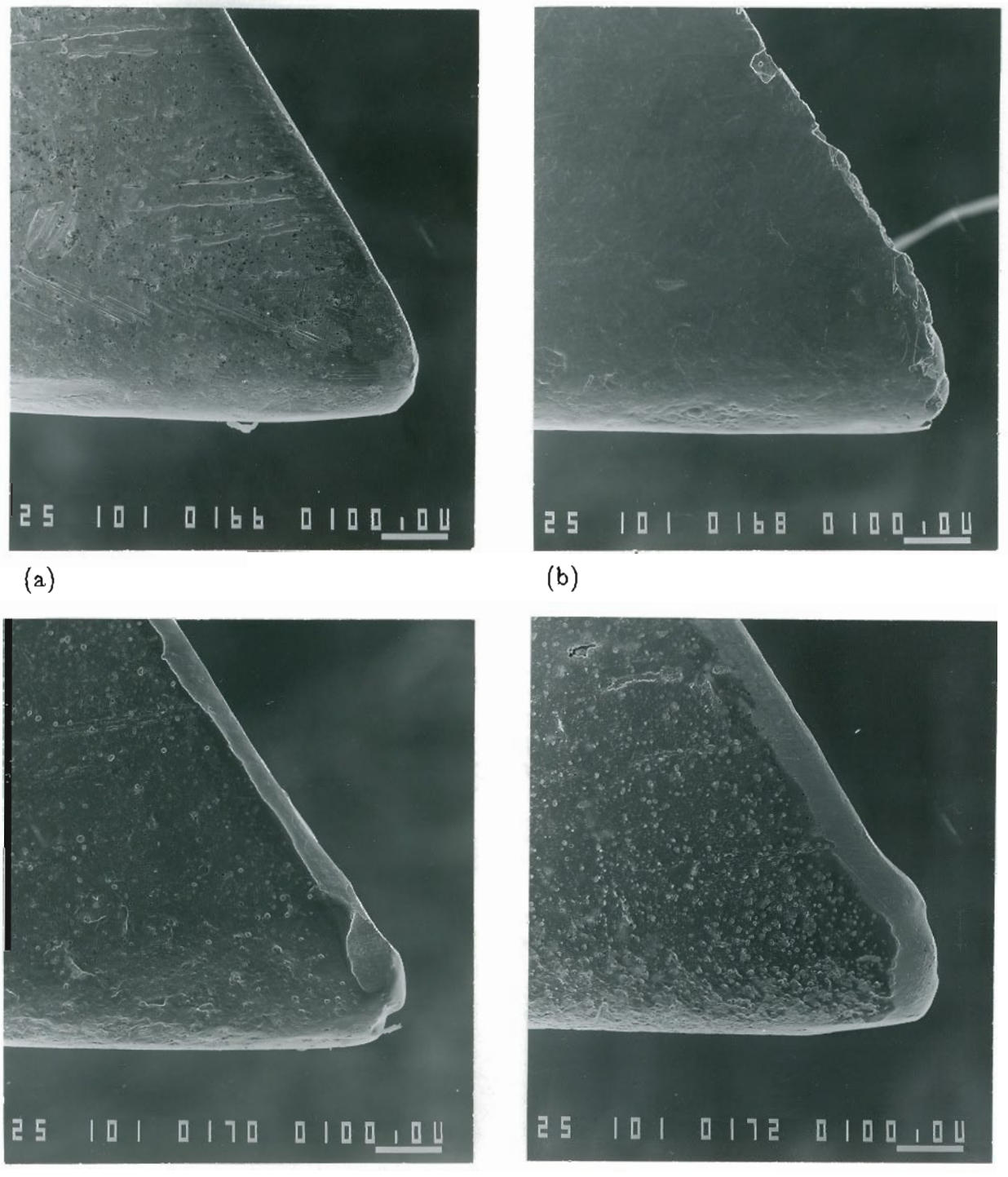

(a) (b)

(c) (d)

Figure 26. Saw chain cutter tips after 5000 ft path length: (a) un-coated, (b) Cr-coated by Omark, (c) TiN-coated by Multi-Arc, and (d) TiN-coated by Balzers.

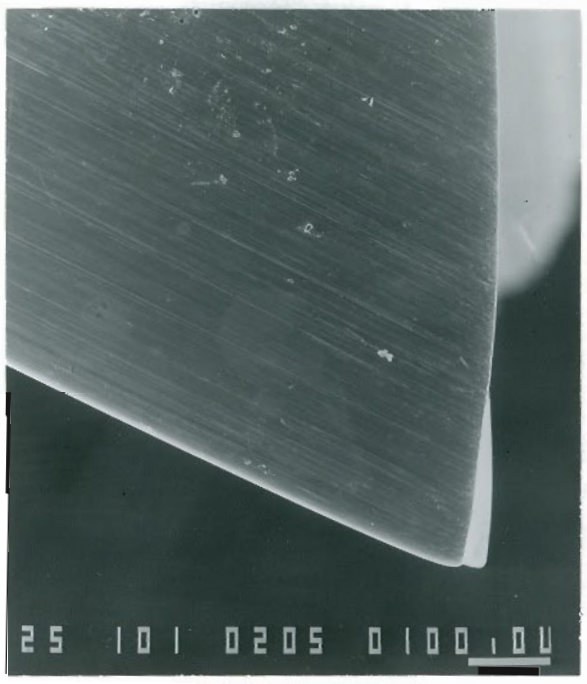

(a)

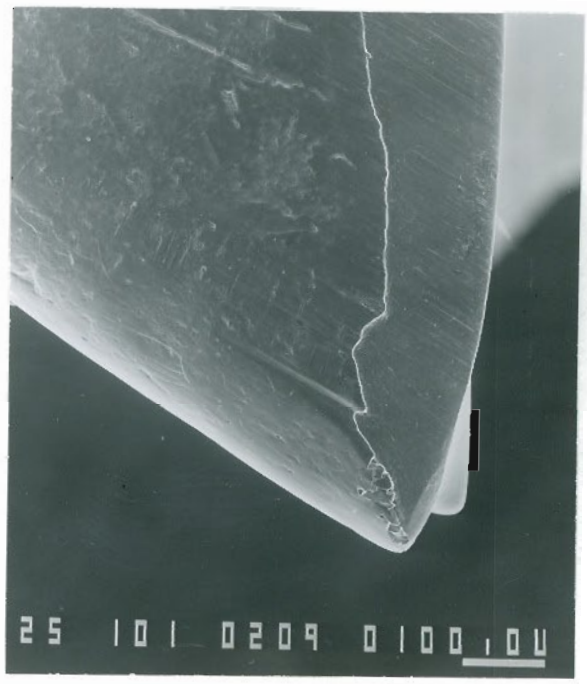

(b)

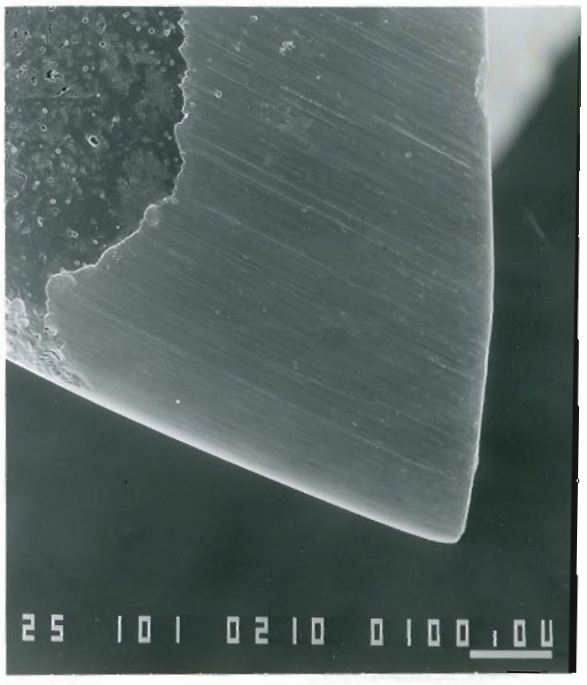

(c)

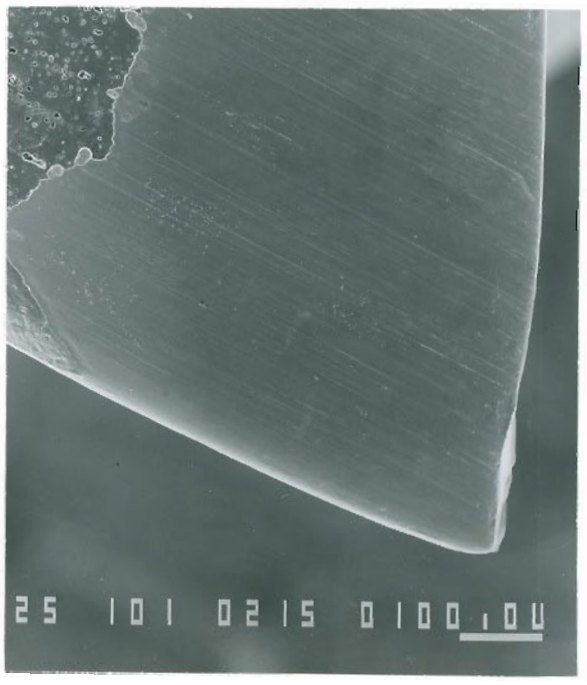

(d)

Figure 27. Saw chain cutter tips after 35,000 ft path length: (a) un-coated, (b) Cr-coated by Omark, (c) TiN-coated by Multi-Arc, and (d) TiN-coated by Balzers.

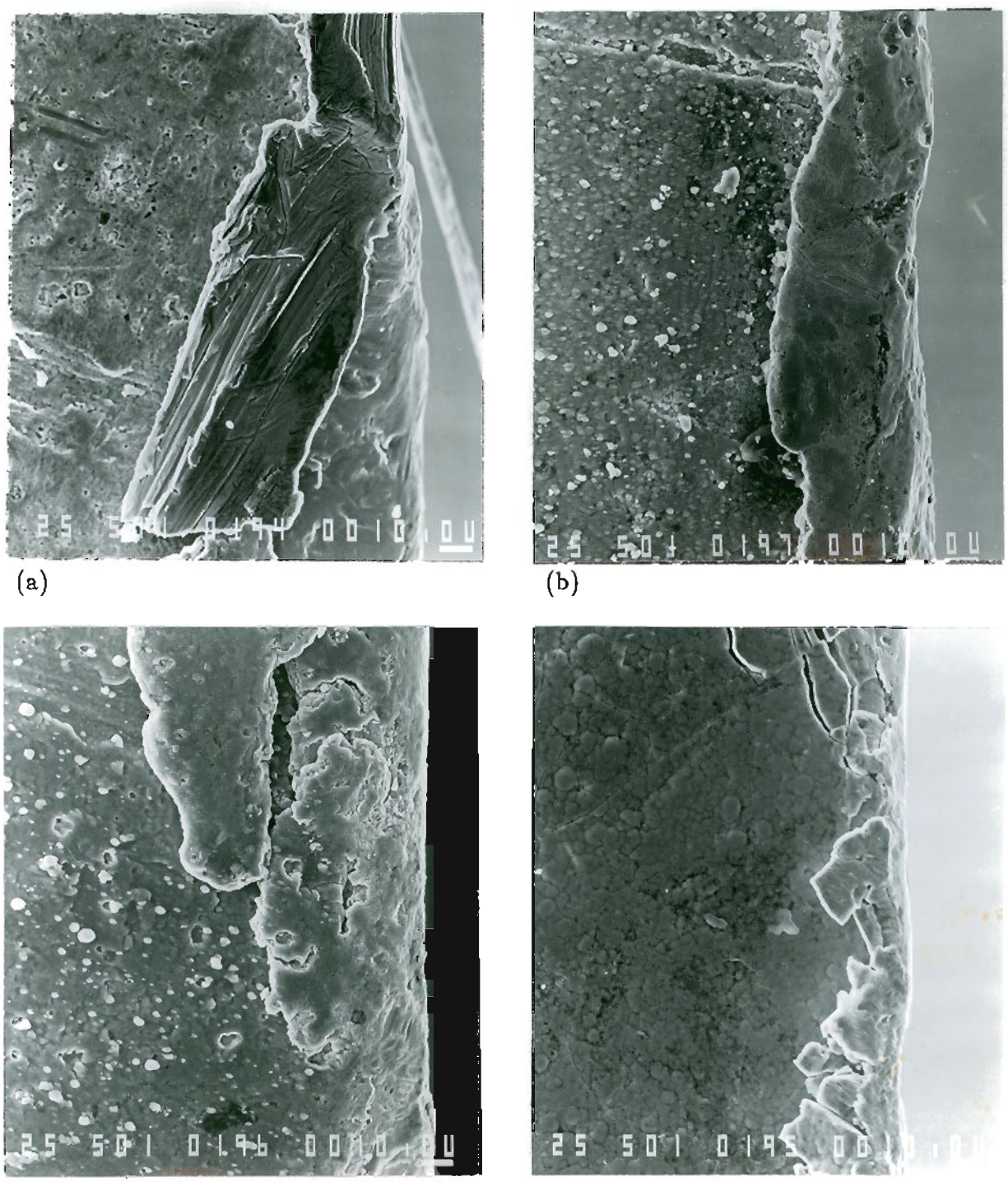

(a) (b)

(c) (d)

Figure 28. Saw chain cutter edges before wear testing: (a) un-coated, (b) Cr-coated by Omark, (c) TiN-coated by Multi-Arc, and (d) TiN-coated by Balzers.

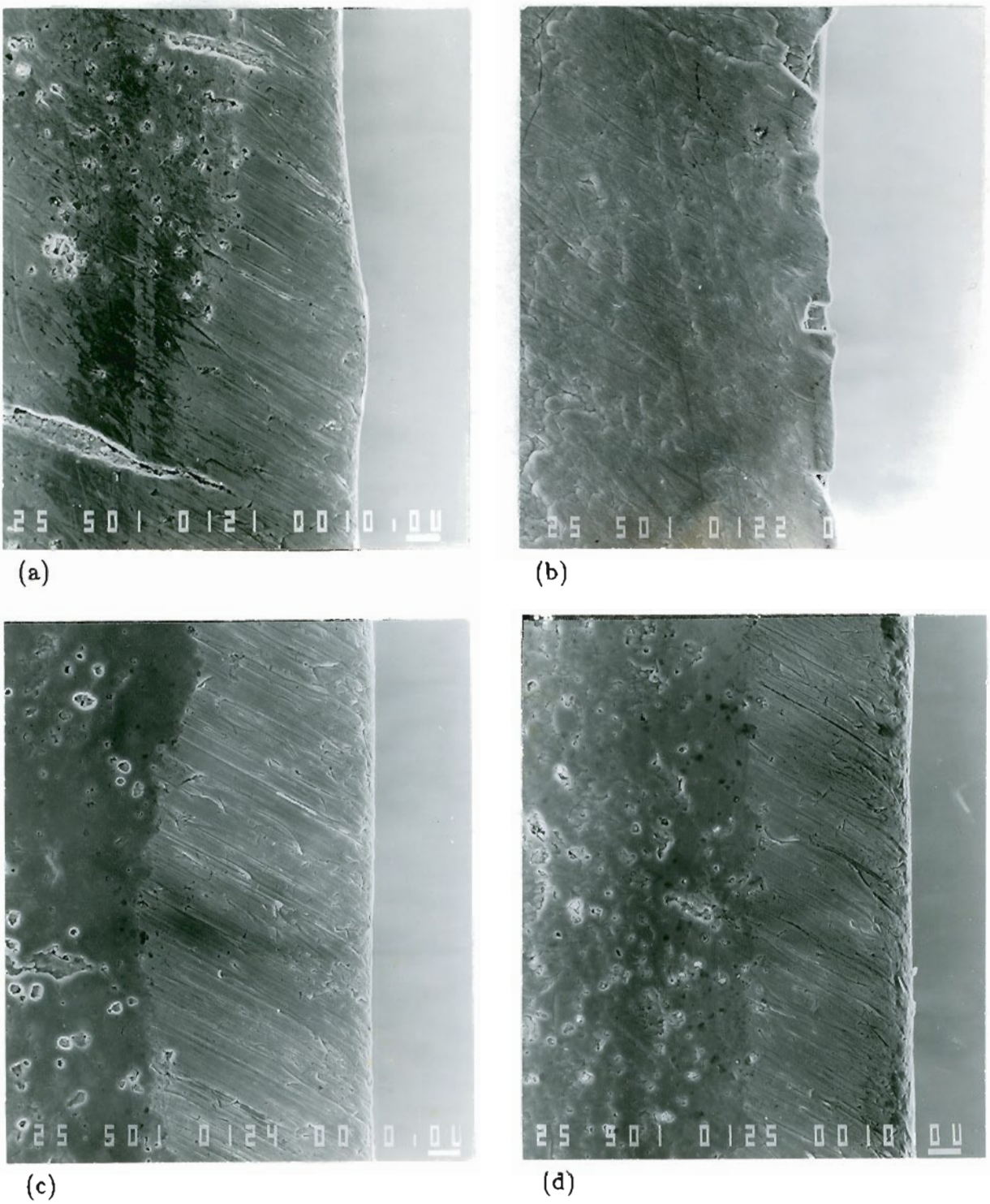

Figure 29. Saw chain cutter edges after 5,000 ft path length: (a) un-coated, (b) Cr-coated by Omark, (c) TiN-coated by Multi-Arc, and (d) TiN-coated by Balzers.

(a)

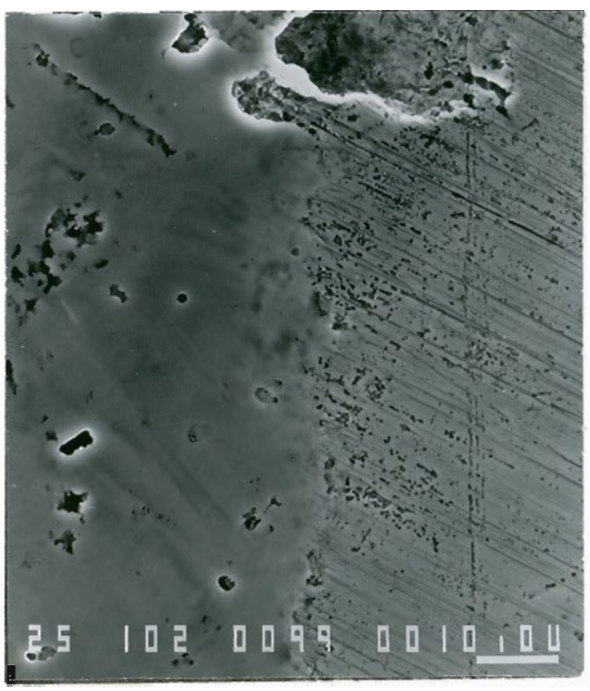

(b)

(c)

Figure 30. Transition between areas of coating removal and remaining coating on saw chain cutters after 35,000 ft path length: (a) Cr-coated by Omark, (b) TiN-coated by Multi-Arc, and (c) TiN-coated by Balzers.

(a)

(b)

(c)

Figure 31. Cross-sections of saw chain cutter clearance face after 35,000 ft path length: (a) Cr-coated by Omark, (b) TiN-coated by Multi-Arc, and (c) TiN-coated by Balzers.

BIOGRAPHICAL NOTE

The author was born in Beijing, China on October 17, 1962. His education career started in September 1969.

The author received his BS degree in Metallurgical Engineering from Hebei Institute of Mechanical and Electrical Engineering in China, in July, 1983. He attended the Academy of Machinery Science and Technology in Beijing, China, as a graduate student in 1983, and earned a MS degree in Metallurgical Engineering in 1986. He had worked for one year for the Academy after graduation.

The author began his study at the Oregon Graduate Institute of Science and Technology in September 1987 and completed the requirement for the degree of Master of Science in Materials Science in August 1989.